

ผลของขนาดอนุภาคของตัวเร่งปฏิกิริยาMFที่มีโลหะแกลเลียมผสมอยู่ต่อการเปลี่ยนเอทานอลเป็นอะโรมาติกส์



นางสาววิภา เตื่อนฉาย

สถาบันวิทยบริการ

จุฬาลงกรณ์มหาวิทยาลัย

วิทยานิพนธ์นี้เป็นส่วนหนึ่งของการศึกษาตามหลักสูตรปริญญาวิศวกรรมศาสตรมหาบัณฑิต

สาขาวิชาวิศวกรรมเคมี ภาควิชาวิศวกรรมเคมี

คณะวิศวกรรมศาสตร์ จุฬาลงกรณ์มหาวิทยาลัย

ปีการศึกษา 2548

ISBN 974-17-5604-6

ลิขสิทธิ์ของจุฬาลงกรณ์มหาวิทยาลัย

EFFECT OF PARTICLE SIZE OF GALLIUM CONTAINING MFI CATALYST  
ON ETHANOL CONVERSION TO AROMATICS



Miss Paweenar Duenchay

สถาบันวิทยบริการ  
จุฬาลงกรณ์มหาวิทยาลัย

A Thesis Submitted in Partial Fulfillment of the Requirements  
for the Degree of Master of Engineering Program in Chemical Engineering

Department of Chemical Engineering

Faculty of Engineering

Chulalongkorn University

Academic Year 2006

ISBN 974-17-5604-6

Thesis Title            EFFECT OF PARTICLE SIZE OF GALLIUM CONTAINING MF  
                                 CATALYST ON ETHANOL CONVERSION TO AROMATICS

By                            Miss Paweenar Duenchay

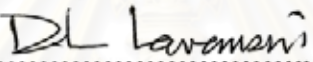
Field of Study            Chemical Engineering

Thesis Advisor            Suphot Phatanasri; D.Eng.

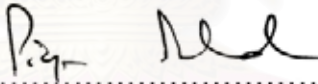
Thesis Co-advisor      Choowong Chaisuk, D.Eng.


---

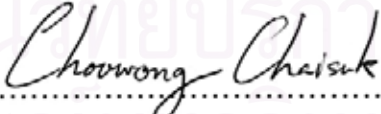
Accepted by the Faculty of Engineering, Chulalongkorn University in Partial  
Fulfillment of the Requirements for the Master's Degree

  
.....Dean of the Faculty of Engineering  
(Professor Direk Lavansiri, Ph.D.)

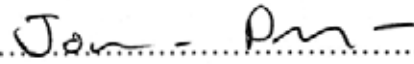
THESIS COMMITTEE

  
.....Chairman  
(Professor Piyasan Praserthdam, Dr.Eng.)

  
.....Thesis Advisor  
(Suphot Phatanasri, D.Eng.)

  
.....Thesis Co-advisor  
(Choowong Chaisuk, D.Eng.)

  
.....Member  
(Assistant Professor Montree Wongsri, D.Sc.)

  
.....Member  
(Assistant Professor Joongjai Panpranot, Ph.D.)

ปวีณา เดือนฉาย: ผลของขนาดอนุภาคของตัวเร่งปฏิกิริยา MFI ที่มีโลหะแกลเลียมผสม  
 อยู่ต่อการเปลี่ยนเอทานอลเป็นอะโรมาติกส์ (EFFECT OF PARTICLE SIZE OF  
 GALLIUM CONTAINING MFI CATALYST ON ETHANOL CONVERSION  
 TO AROMATICS) อ. ที่ปรึกษา: ดร.สุพจน์ พัฒนะศรี, อ.ที่ปรึกษาร่วม: ดร.ชวงค์ ชัยสุข,  
 84 หน้า. ISBN: 974-17-5604-6

งานวิจัยนี้มีวัตถุประสงค์เพื่อทำการศึกษากลไกของขนาดอนุภาคของตัวเร่งปฏิกิริยา MFI ที่มีโลหะแกลเลียมผสม ต่อประสิทธิภาพในการสังเคราะห์อะโรมาติกส์จากเอทานอล โดยการสังเคราะห์ MFI ซีโอไลต์ที่มีอัตราส่วน  $\text{SiO}_2/\text{Al}_2\text{O}_3$  เท่ากับ 40 โดยมีขนาดอนุภาคต่างๆกัน 5 ขนาดดังนี้ 1.0, 1.9, 3.2, 4.1 และ 6.0 ไมโครเมตร ด้วยวิธีการไฮโดรเทอร์มอล แล้วผสมโลหะแกลเลียมด้วยวิธีแลกเปลี่ยนไอออน และทำการปรับสภาพด้วยน้ำและความร้อน แล้วทำการวิเคราะห์คุณลักษณะของซีโอไลต์ที่เตรียมขึ้นด้วยเทคนิค XRD, XRF, BET, SEM,  $\text{NH}_3$ -TPD และ  $^{27}\text{Al}$  MAS NMR จากผลการศึกษาจะพบว่าภายหลังจากภาวะที่มีน้ำและความร้อนสูง ตัวเร่งปฏิกิริยาที่มีอนุภาคขนาดเล็กจะสูญเสียความเป็นผลึก ความเป็นกรด และปริมาณอลูมิเนียมในโครงสร้างลดลงเล็กน้อย ในขณะที่ตัวเร่งปฏิกิริยาที่มีอนุภาคขนาดใหญ่จะสูญเสียความเป็นผลึก ความเป็นกรด และปริมาณอลูมิเนียมในโครงสร้างมากกว่า การทดสอบตัวเร่งปฏิกิริยาต่อประสิทธิภาพในการสังเคราะห์อะโรมาติกส์จากเอทานอล พบว่าแกลเลียมมีผลต่อการเกิดอะโรมาติกส์มากกว่าความเป็นกรด ในขณะที่ความเป็นกรดส่งผลต่อการเลือกเกิดของเบนซีน โทลูอีน ไซลีน และพบว่าตัวเร่งปฏิกิริยา MFI ที่มีโลหะแกลเลียมผสมทั้งก่อนและหลังการผ่านภาวะที่มีน้ำและความร้อนสูง มีความเป็นกรดมากพอที่จะเกิดสารกลุ่มโอเลฟิน

## สถาบันวิทยบริการ จุฬาลงกรณ์มหาวิทยาลัย

ภาควิชา.....วิศวกรรมเคมี..... ลายมือชื่อนิสิต..... ปวีณา เกื้อนคาน  
 สาขาวิชา.....วิศวกรรมเคมี..... ลายมือชื่ออาจารย์ที่ปรึกษา..... Jim Wong  
 ปีการศึกษา.....2548..... ลายมือชื่ออาจารย์ที่ปรึกษาร่วม..... [Signature]

##4770589621 : MAJOR CHEMICAL ENGINEERING

KEY WORDS: PARTICLE SIZE / MFI ZEOLITE / ETHANOL AROMATIZATION

PAWEENAR DUENCHAY: EFFECT OF PARTICLE SIZE OF GALLIUM CONTAINING MFI CATALYST ON ETHANOL CONVERSION TO AROMATICS. THESIS ADVISOR: SUPHOT PHATANASRI, D.Eng., THESIS CO-ADVISOR: CHOOWONG CHAISUK, D.Eng. 84 pp. ISBN 974-17-5604-6

Effect of particle size of gallium containing MFI catalyst on ethanol conversion to aromatics was investigated in this research. Five of MFI zeolite catalysts, having different particle size (1.0, 1.9, 3.2, 4.1 and 6.0  $\mu\text{m}$ ), were synthesized by hydrothermal treatment with  $\text{SiO}_2/\text{Al}_2\text{O}_3$  ratios of 40. Gallium were contained on these catalysts by ion-exchanged. The obtained products were characterized by XRD, XRF, BET, SEM,  $\text{NH}_3$ -TPD and  $^{27}\text{Al}$  MAS NMR spectrometer. After these catalysts were pretreated, the results suggest that the small particle size of Ga/MFI catalysts showed a slight decrease in crystallinity, moderate acidity and moderate dealumination of tetrahedral aluminum while the large particle size of Ga/MFI catalysts lost considerable crystallinity, extensive acidity and extensive dealumination. The influence of catalysts on ethanol conversion aromatics were examined three points; gallium affected to the selectivity of aromatics more than acidity, the acidity affected to the selectivity of 1) benzene 2) toluene 3) xylene and the acidity of all Ga/MFI (fresh and pretreated) catalysts was enough to convert ethanol to olefins.

สถาบันวิทยบริการ  
จุฬาลงกรณ์มหาวิทยาลัย

Department.....Chemical Engineering...

Field of study...Chemical Engineering...

Academic year.....2005.....

Student's signature... *Paweenar Duenchay*

Advisor's signature... *Suphot Phatanasri*

Co-Advisor's signature... *Choowong Chaisuk*

## ACKNOWLEDGEMENTS

The author would like to express her greatest gratitude to her advisor, Dr. Suphot Phatanasri, for his invaluable guidance, useful discussions, and warm encouragement throughout this study. She wishes to give her gratitude to Dr. Choowong Chaisuk, the thesis co-advisor, for his kind guidance and encouragement. In addition, the author would also grateful to Professor Piyasan Prasertdam, as the chairman and Assistant Professor Montree Wongsri, and Assistant Professor Joongjai Panpranot as the member of the thesis committee. The financial support of the Thailand Search Fund (TRF) and the Graduate School of Chulalongkorn University are gratefully acknowledged.

Most of all, the author would like to express her highest gratitude to her parents who always pay attention to her all the times for suggestions and have provided her support and encouragement. The most success of graduation is devoted to her parents.

Finally, the author wishes to thank the members of the Center of Excellence on Catalysis Reaction Engineering, Department of Chemical Engineering, faculty of Engineering, Chulalongkorn University for their assistance especially Mr.Watcharapong Khaodee.

สถาบันวิทยบริการ  
จุฬาลงกรณ์มหาวิทยาลัย

# CONTENTS

	<b>page</b>
<b>ABSTRACT (IN THAI)</b> .....	iv
<b>ABSTRACT (IN ENGLISH)</b> .....	v
<b>ACKNOWLEDGEMENTS</b> .....	vi
<b>CONTENTS</b> .....	vii
<b>LIST OF TABLES</b> .....	x
<b>LIST OF FIGURES</b> .....	xi
<b>CHAPTER</b>	
<b>I INTRODUCTION</b> .....	1
1.1 Research objectives .....	2
1.2 Research Scopes .....	2
<b>II LITERATURE REVIEWS</b> .....	4
<b>III THEORY</b> .....	8
3.1 Structure of Zeolite.....	8
3.2 Category of Zeolite.....	11
3.3 Zeolite Active sites.....	17
3.3.1 Acid sites.....	17
3.3.2 Generation of Acid Centers.....	18
3.3.3 Basic sites.....	21
3.4 Shape Selective.....	22
3.5 Zeolite Synthesis.....	23
3.6 Aromatics.. ..	25
3.7 Reaction Mechanism of Ethanol to Aromatics .....	25
<b>IV EXPERIMENTS</b> .....	28
4.1 Catalyst preparation.....	28
4.1.1 Chemicals.....	28
4.1.2 Preparation of NaZSM-5 ( MFI) .....	28
4.1.2.1 Preparation of Gel Precipitation and Decantation Solution.....	31
4.1.2.2 Crystallization.....	31

<b>CHAPTER</b>	<b>page</b>
4.1.2.3 Calcination .....	32
4.1.2.4 Ammonium ion-exchange.....	32
4.1.3 Gallium loading by ion-exchanged.....	33
4.2 Pretreatment condition.....	33
4.3 Characterization .....	33
4.3.1 X-Ray Diffraction analysis (XRD).....	33
4.3.2 X-Ray Fluorescence analysis (XRF).....	34
4.3.3 BET surface area measurement.....	34
4.3.4 Scanning Electron Microscopy (SEM).....	34
4.3.5 <sup>27</sup> Al Magnetic Angle Spinning Nuclear Magnetic Resonance ( <sup>27</sup> Al MAS NMR).....	34
4.3.6 Temperature Programmed Adsorptions of Ammonia (NH <sub>3</sub> -TPD) .....	35
4.3 Reaction Testing.....	35
4.3.1 Chemicals and Reagents.....	35
4.3.2 Instruments and Apparatus.....	35
4.3.3 Reaction Method.....	37
<b>V RESULTS AND DISCUSSION.....</b>	<b>39</b>
5.1 Characterization of the catalysts.....	39
5.1.1 X-Ray Diffraction pattern .....	39
5.1.2 Morphology.....	40
5.1.3 Physical Properties.....	46
5.1.4 Dealumination.....	46
5.1.5 Temperature Programmed Adsorptions of Ammonia (NH <sub>3</sub> -TPD) .....	51
5.2 Catalytic Reaction .....	55
5.2.1 The effect of acidity and Gallium on the selectivity of aromatics.....	55
5.2.2 The effect of acidity on the selectivity of aromatics(BTX) ...	56
5.2.3 The effect of acidity on the selectivity of olefins.....	56



<b>CHAPTER</b>	<b>page</b>
<b>VI CONCLUSIONS AND RECOMMENDATIONS</b> .....	59
<b>REFERENCES</b> .....	61
<b>APPENDICES</b> .....	
<b>Appendix A SAMPLE OF CALCULATIONS</b>	65
<b>A-1</b> Calculation of Si/Al Atomic Ratio for MFI .....	65
<b>A-2</b> Calculation of the amount of Ga ion-exchanged MFI.....	66
<b>A-3</b> Calculation of particle size from SEM photograph.....	66
<b>A-4</b> Calculation of vapor pressure of water.....	67
<b>A-5</b> Calculation of percent crystallinity .....	68
<b>A-6</b> Calculation of the relative area of tetrahedral aluminum (%)...	68
<b>Appendix B</b> CALCULATIONS OF REACTION FLOW RATE.....	69
<b>Appendix C</b> DATA OF EXPERIMENT.....	70
<b>Appendix D</b> LIST OF PUBLICATION.....	78
<b>VITAE</b> .....	84

## LIST OF TABLES

TABLE	page
3.2 Structural characteristics of selected zeolites.....	12
4.1 The chemicals used in the catalyst preparation .....	28
4.2 Reagents used for the preparation of Na/MFI: Si/Al = 40.....	29
4.3 Operating condition for gas chromatograph.....	36
5.1 Physical properties of various particle sizes of Ga/MFI catalysts.....	47
5.2 The peak concentration of acid sites of the various particle size .....	51
C.1 Product distribution on ethanol aromatization with various particle sizes (a) fresh catalysts (b) pretreated catalysts.....	74



สถาบันวิทยบริการ  
จุฬาลงกรณ์มหาวิทยาลัย

## LIST OF FIGURES

FIGURE	page
3.1 TO <sub>4</sub> tetrahedra (T=Si or Al).....	9
3.2 Secondary building units (SBU's) found in zeolite structures.....	10
3.3 Structure of ZSM-5.....	13
3.4 Structure of Faujasite.....	14
3.5 Structure of Beta zeolite.....	14
3.6 Structure of zeolite ZSM-12 .....	15
3.7 Structure of Mordenite.....	16
3.8 Framework structure of MCM-22 .....	17
3.9 Diagram of the surface of a zeolite framework.....	19
3.10 Water molecules co-ordinated to polyvalent cation are dissociated by heat treatment yielding Brønsted acidity.....	20
3.11 Lewis acid site developed by dehydroxylation of Brønsted acid site.....	20
3.12 Steam dealumination process in zeolite.....	21
3.13 The enhancement of the acid strength of OH groups by their interaction with dislodged aluminum species.....	22
3.14 Diagram depicting the three type of selectivity.....	23
3.15 Aromatics.....	25
4.1 The preparation procedure of MFI by rapid crystallization method .....	38
4.2 Schematic diagram of the reaction apparatus for reaction .....	39
5.1 X-ray Diffraction patterns of commercial MFI zeolite.....	40
5.2 X-ray Diffraction patterns of Ga/MFI catalysts .....	41
5.3 X-ray Diffraction patterns of Ga/MFI catalysts pretreated at 800 °C with 10% H <sub>2</sub> O for 24 h .....	42
5.4 Scanning electron micrograph of H/MFI (1.9 μm) catalyst .....	43
5.5 Scanning electron micrograph of Ga/MFI (1.0 μm) catalyst .....	43
5.6 Scanning electron micrograph of Ga/MFI (1.9 μm) catalyst .....	44
5.7 Scanning electron micrograph of Ga/MFI (3.2 μm) catalyst .....	44

<b>FIGURE</b>	<b>page</b>
5.8 Scanning electron micrograph of Ga/MFI (4.1 $\mu\text{m}$ ) catalyst .....	45
5.9 Scanning electron micrograph of Ga/MFI (6.0 $\mu\text{m}$ ) catalyst .....	45
5.10 $^{27}\text{Al}$ MAS NMR spectra of Ga/MFI (a) fresh and (b) pretreated .....	48
5.11 The effect of particle size on the relative loss of crystallinity .....	50
5.12 The effect of particle size on the relative loss of tetrahedral aluminum.....	50
5.13 The Temperature Programmed Desorption Profile of fresh Ga/MFI catalysts for various particle sizes (a) 1.0 $\mu\text{m}$ (b) 1.9 $\mu\text{m}$ (c) 3.2 $\mu\text{m}$ (d) 4.1 $\mu\text{m}$ (e) 6.0 $\mu\text{m}$ .....	52
5.14 The Temperature Programmed Desorption Profile of pretreated Ga/MFI catalysts for various particle sizes (a) 1.0 $\mu\text{m}$ (b) 1.9 $\mu\text{m}$ (c) 3.2 $\mu\text{m}$ (d) 4.1 $\mu\text{m}$ (e) 6.0 $\mu\text{m}$ .....	53
5.15 The effect of particle size on the relative loss of acidity .....	54
5.16 The effect of acidity and Gallium on the selectivity of aromatics.....	55
5.17 The selectivity of fresh catalyst on ethanol aromatization.....	56
5.18 The selectivity of pretreated catalyst on ethanol aromatization.....	57
A1 Scanning electron micrograph of H/MFI (2.0 $\mu\text{m}$ ) catalyst.....	66
C1 Calibration curve of Ethanol.....	75
C2 Calibration curve of Benzene.....	75
C3 Calibration curve of Toluene.....	76
C4 Calibration curve of o-xylene.....	76
C5 Calibration curve of m-xylene.....	77
C6 Calibration curve of p-xylene.....	77

# CHAPTER I

## INTRODUCTION

Conversion of methanol and ethanol to gasoline and other hydrocarbons has received wide attention these days due to the global energy crisis and the heavy demand for aromatic hydrocarbons. Both the raw materials hold good promise – methanol can be obtained in large quantities from natural gas and ethanol can be obtained from fermentation of biomass, a renewable agricultural resource. Countries like Thailand and India, which have large sugarcane and cassava cultivation, can produce ethanol easily from fermentation of molasses, a by product of sugar industry. A profitable way to increase the value of the raw material present in such petroleum feedstock is to transform them directly into aromatic products which have high octane number and have a wide variety of applications in the petrochemical and chemical industries. They are important raw materials for many intermediates of commodity petrochemicals and valuable fine chemicals, such as monomers for polyesters, engineering plastics, intermediates for detergents, pharmaceuticals, agricultural-products and explosives. Among them, benzene, toluene and xylenes (BTX) are the three basic materials for most intermediates of aromatic derivatives (Wittcoff, H.A.,1992).

The zeolite MFI catalysts doped with gallium and also with other compounds such as zinc, platinum and bimetallics have long been used for conversion of methanol and C<sub>3</sub>-C<sub>4</sub> liquefied petroleum gas (LPG) into aromatic hydrocarbons. The nature of the product depends on a number of factors, a notable factor being the concentration of brønsted acid sites on the catalyst. With an increase in the number of acid sites, achieved by low Si/Al ratio, there is a definite selectivity trend towards the aromatics. There have been only a few studies of the conversion of ethanol into aromatics and effect of particle size of the zeolite MFI catalysts doped with gallium. Therefore, this research aims to investigate the catalytic performance of various particle sizes of the zeolite MFI catalysts doped with gallium on ethanol aromatization.

## 1.1 Research objectives

The objective of this research is to investigate the characteristics and performance of the prepared difference particle sizes gallium containing MFI-type zeolite catalysts on aromatization of ethanol.

## 1.2 Research Scopes

1. Study the method to synthesis and introduction of gallium into MFI-type zeolite catalyst.
2. Study the characterization of the prepared catalysts by the following methods.
  - Analyzing structure and crystallinity of catalysts by X-ray diffraction (XRD).
  - Analyzing amount of metal of catalysts by X-ray fluorescence (XRF).
  - Analyzing shape and size of crystallites by Scanning Electron Microscope (SEM).
  - Analyzing surface areas of catalysts by Brunauer-Emmett-Teller (BET) surface areas measurement.
  - Analyzing the acidity of catalysts by  $\text{NH}_3$ -TPD
3. Investigate the performance of the prepared catalysts on the aromatization of ethanol under the following condition.
  - Atmospheric pressure.
  - Reaction temperature  $600\text{ }^\circ\text{C}$
  - Space velocity  $2,000\text{ h}^{-1}$
  - Reactant feed 20% ethanol and 80% nitrogen, as diluents

The reaction products were analyzed by Gas Chromatographs

This thesis is arranged as follows:

Chapter II presents literature reviews of previous works related to this research.

Chapter III explains basic information about zeolite and metal containing MFI catalysts

Chapter IV describes synthesis of various particle sizes of the MFI zeolite catalyst doped with gallium on ethanol aromatization employed in this research and experimental apparatus.

Chapter V presents experimental results and discussion.

Chapter VI presents overall conclusions of this research and recommendations for future research.



สถาบันวิทยบริการ  
จุฬาลงกรณ์มหาวิทยาลัย

## CHAPTER II

### LITERATURE REVIEWS

In 1972, Mobil Oil Corp. published zeolite “ZSM-5” that is the catalyst which synthesized gasoline shape-selectivity from methane (The MTG process). A lot of laboratory has been developed. Some of the more prominent studied on modified catalysts and the process performance are summarized below.

Zaihui Fu et al. (1995) reported the modified ZSM-5 catalysts for propane aromatization prepared by a solid state reaction. A solid-exchange mechanism is suggested that Zn. ZSM-5 is the most active catalysts for propane conversion and gives a better benzene, toluene and xylenes selectivity. Other Mo-ZSM-5, propane mainly undergoes cracking to methane and ethane, and the loading ZSM-5 with  $\text{Cr}^{5+}$  enhances the propane dehydrogenation to propene.

Yoshihiro Inoue et al. (1995) reported the introduction of  $\text{Ag}^+$  ions into ZSM-5 zeolites appreciably enhances the selectivity for aromatic hydrocarbons in the conversion of methanol. Thus, the yield of aromatics over H-ZSM-5 and Ag- ZSM-5 was 43% and 80% respectively, at 1023°C. The distribution of aromatics over Ag-ZSM-5 at 1023°C was 3, 12, 36 and 12% for benzene, toluene, xylenes plus ethylbenzene and  $\text{C}_{10+}$ , respectively. It is concluded that  $\text{Ag}^+$  ions have a capability of efficiently converting alkene intermediates into aromatic hydrocarbons.

Lee et al. (1995) investigated the interaction between gallium and H-ZSM-5 on gallium supported H-ZSM-5 catalysts. Gallium was introduced into H-ZSM-5 by impregnation [Ga/Z5 (im)] and physical mixing [Ga/Z5 (mix)]. Temperature-programmed adsorptions studies of ammonia show that the number of strong acid sites (HTP) of H-ZSM-5 decreased after hydrogen pretreatment, while the number of weak acid site (LTP) increased at the same time. The fall of the HTP is compensated for by the rise of the LTP. If the pretreatment time was long enough, the HTP would disappear completely. The new acid center (Ga-Z) was also an active site for acid catalyzed reaction (cracking, oligomerization and cyclization) as H-Z. The main



factor affecting the catalytic activity was the dispersion of gallium rather than the oxidation state. The yield of aromatics on the reduced and reoxidized catalysts were similar. On hydrogen pretreatment, the residual gallium species (probably in the form of  $\text{Ga}_2\text{O}$ ) sinter and block the aperture and/or the internal channel of zeolite. Because Ga/Z5 (im) sintered more seriously than Ga/Z5 (mix) were superior to those of Ga/Z5 (im), especially at higher space velocity.

Chau-Sang Chang and Min-Dar Lee (1995) studied the hydrogen pretreatment effect on catalytic properties of Ga/ZSM-5. The interaction between gallium and H-ZSM-5 can improve the dispersity of gallium and at the same time increase the activity for aromatization of n-hexane from 44.2 to 60.3% with simultaneous decrease of the selectivity to aliphatics.

Viswanadham, N., et al. (1996) studies the effect of the dehydrogenating component of H-ZSM-5 and Zn/ H-ZSM-5 catalysts on n-heptane aromatization reaction. Incorporation of zinc enhances the concentration of olefin precursors through its effective dehydrogenation action on paraffins, which ultimately results in enhancement in aromatic yield. Zinc also facilitates the formation of  $\text{C}_6\text{-C}_8$  aromatics from the corresponding oligomers, as in that way suppresses the formation of  $\text{C}_9\text{-C}_{12}$  oligomers, a source for the formation of higher ( $\text{C}_{9+}$ ) aromatics.

Kumar, N. and Lindfors, L.E., (1996) investigated modification of the ZSM-5 zeolite using Ga and Zn impregnated silica fibre for the conversion of n-butane into aromatic hydrocarbon. In this work a silica fibre pre-impregnated with Ga and Zn has been used during the synthesis by which Ga-ZSM-5 and Zn-ZSM-5 zeolite catalysts were prepared. The catalysts synthesized consisted of Brønsted and Lewis types of acid sites with uniform dispersion of Ga and Zn cation. The catalysts were found to be very active for n-butane conversion and for transformation into aromatic hydrocarbons. The Ga and Zn cation balanced together with Brønsted acid sites were the active sites for this reaction. The deactivation due to coke formation was very low for the Ga and Zn modified zeolite catalysts.

Kumar N., et al. (1997) investigated aromatization of n-butane over Ni-ZSM-5 and Cu-ZSM-5 zeolite catalysts prepared by using Ni and Cu impregnated

silica fiber. It found that the modification of the ZSM-5 by Ni and Cu increased the selectivity to aromatic hydrocarbons. The state of Ni and Cu and their stabilization in ZSM-5 structure was highly influenced by the mode of catalyst pretreatment.

Choudhary, V.R., et al. (1997) studied direct aromatization of natural gas over H-gallosilicate (MFI), H-galloaluminosilicate (MFI) and Ga/H-ZSM-5 zeolite. They found that direct conversion of the C<sub>2+</sub>hydrocarbons from nature gas to aromatics over H-gallosilicate (MFI), H-galloaluminosilicate (MFI) and Ga/H-ZSM-5 zeolite has been investigated at different temperatures (500-600°C) and space velocities (500-6000 cm<sup>3</sup>g<sup>-1</sup>h<sup>-1</sup>). The zeolites are compared for their activity/selectivity and distribution of aromatics formed in the natural gas-to-aromatics conversion at different process conditions. The performance show by the zeolites is in the following order: H-galloaluminosilicate (MFI) >> H-gallosilicate (MFI) > Ga/H-ZSM-5. Natural gas, containing 27.3% C<sub>2+</sub>hydrocarbons, can be converted to aromatica with very high selectivity (~90%) at high conversion (70%) of C<sub>2+</sub>hydrocarbons over H-galloaluminosilicate (MFI) zeolite at 600°C and space velocities of 3000 cm<sup>3</sup>g<sup>-1</sup>h<sup>-1</sup>.

Hu Zeshan et al. (1998) studies the modification of HZSM-5 by metal surfactant for aromatization of methylcyclohexane. The modification resulted in an increase in external surface area, a slight decrease in pore window and gave almost unchanged micropore volume as well as internal surface area. Both conversion and selectivity of aromatization were increase by the modification with zinc valerate, while also resulted in an improment in shape selectivity of the zeolite. There existed an optimal zinc ion ratio of external surface/internal surface of the zeolite for aromatization. The ratio can be obtained by a combination of zinc valerate modification and zinc ion exchange. The modification with magnesium valerate, however, resulted in a decrease of C<sub>1</sub>-C<sub>4</sub> hydrocarbon selectivity and its yield.

Vasant R. Choudhary et al. (2000) studies influence of zeolite factors affecting zeolitic acidity on the propane aromatization activity and selectivity of Ga/H-ZSM-5. They found that the acidity of Ga/H-ZSM-5 zeolite catalyst is strongly influenced by its Si/Al ratio and degree of H<sup>+</sup> exchange and calcinations temperature but not by its Ga loading. As expected, the acidity is increase with increasing degree

of  $H^+$  exchange and it is decrease with increasing Ga loading, but the decrease is small. At high Ga loading, only a small part of the gallium may exist as  $GaO^+$  or  $Ga^+$  and there is little or on possibility of the existence of  $Ga^{3+}$  species in the zeolite channels. Both the conversion of propane and product selectivity are substantially influenced by the Si/Al ratio, degree of  $H^+$  exchange, calcinations temperature and Ga loading of the zeolite catalyst, the propane conversion/aromatization activity. However, for the zeolite catalyst with higher Ga loading, but somewhat lower acidity, the propane conversion/aromatization activity is higher. Thus, for a better performance in the propane aromatization there should be a proper balance between the acidity and Ga species in the zeolite channel.

Choudhary, V.R., et al. (2003) investigated influence of zeolite acidity (strong acid sites measured in terms of the pyridine chemisorbed at  $400^\circ C$ ) and non-framework Ga-species present in the zeolite channels on the conversion ( total and to aromatics) and selectivity in the aromatization of n-heptane at  $500^\circ C$  over the H-AIMFI (H-ZSM-5), Ga/H-AIMFI, H-GaMFI and H-GaAIMFI zeolite catalysts (GHSV = 3400 and 13,600  $h^{-1}$ ). Among the zeolite catalysts, the H-GaAIMFI (with high acidity and high non-FW Ga) showed the highest n-heptane conversion and aromatization activity. Both the zeolitic acidity and non-FW Ga-species were found to play important role in the aromatization process, producing a combined effect.

Choudhary, T.V., et al. (2004) investigated the influence of temperature on the product selectivity, aromatics distribution, p-X/o-X and p-X/m-X product ratio, aromatization/cracking and aromatization/dehydrogenation ratio have been exhaustively on H-GaAIMFI at different isoconversion of propane. There studies show a profound influence of temperature on the product selectivity/distribution of the propane aromatization reaction. The aromatization activity of the H-GaAIMFI zeolite decreases at higher temperatures relative to the creaking and dehydrogenation activities. The benzene selectivity and the formation of xylene isomers are kinetically controlled.

## CHAPTER III

### THEORY

#### 3.1 The structure of the zeolite

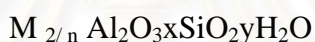
Zeolites are highly crystalline, hydrated aluminosilicates that upon dehydration develop in the ideal crystal a uniform pore structure having minimum channel diameters (aperture) of from about 0.3 to 1.0 nm. The size depends primarily on the type of zeolites and secondarily on the cations present and the nature of treatments such as calcination, leaching, and various chemical treatments. Zeolites have been of intense interest as catalysts for some three decades because of the high activity and unusual selectivity they provide, mostly in a variety of acid-catalyzed reactions. In many cases, but not all, the unusual selectivity is associated with the extremely fine pore structure, which permits only certain molecules to penetrate into the interior of the catalyst particles, or only certain products to escape from the interior. In some cases unusual selectivity seems to stem instead from constraints that the pore structure sets on allowable transition states, sometimes termed spacio – selectivity.

The structure of the zeolite consists of a three-dimensional framework of the  $\text{SiO}_4$  and  $\text{AlO}_4$  tetrahedra as presented in Figure 3.1 (King, R.B., 1994), each of which contains a silicon or aluminum atom in the center. In 1982, Barrer defined zeolites as the porous tectosilicates (Barrer, R.B., 1982), that is, three-dimensional networks built up of  $\text{TO}_4$  tetrahedra where T is silicon or aluminum. The oxygen atoms are shared between adjoining tetrahedra, which can be present in various ratios and arranged in a variety of ways. The framework thus obtained has pores, channels, and cages, or interconnected voids.

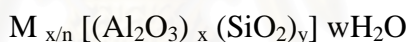
A secondary building unit (SBU) consists of selected geometric groupings of those tetrahedra. There are sixteen such building units, which can be used to describe all of known zeolite structures; for example, 4 (S4R), 6 (S6R), and 8 (S8R) – member single rings, 4-4 (D6R), 8-8 (D8R)-member double rings. The topologies of these

units are shown in Figure 3.2 (Bekkum et al., 1991). Also listed are the symbols used to describe them. Most zeolite framework can be generated from several different SBU's. Descriptions of known zeolite structures based on their SBU's (Szoztak, R,1989). Both ZSM-5 zeolite and Ferrierite are described by their 5-1 building units. Offertile, Zeolite L, Cancrinite, and Erionite are generated using only single 6-member rings. Some zeolite structures can be described by several buildings. The sodalite framework can be built from either the single 6-member ring or the single 4-member ring. Faujasite (type X or type Y) and zeolite be constructed using 4 ring or 6 ring building units. Zeolite a can also be formed using double 4 ring building units, whereas Faujasite cannot.

Zeolites may be represented by the empirical formula:



or by a structural formula:



Where the bracketed term is the crystallographic unit cell. The metal cation (of valencen) is present it produces electrical neutrality since for each aluminum tetrahedron in the lattice there is an overall charge of  $-1$ . Access to the channels is limited by aperture consisting of a ring of oxygen atoms of connected tetrahedra. There may be 4, 5, 6, 8, 10, or 12 oxygen atoms in the ring. In some cases an interior cavity exists of larger diameter in the aperture; in others, the channel is of uniform diameter like a tube (Satterfield,C.N.,1991).

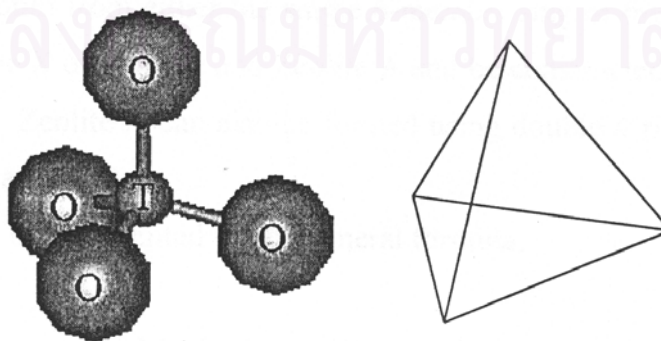


**Figure 3.1**  $TO_4$  tetrahedra (T=Si or Al ) (King,R.B., 1994)

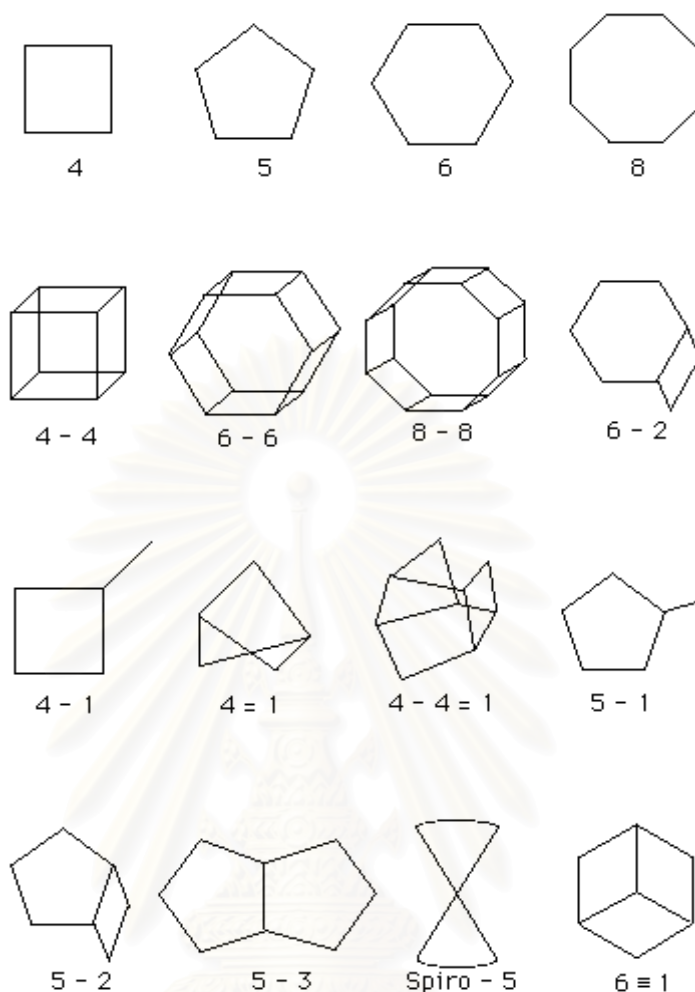


**Figure 3.2** Secondary building units (SBU's) found in zeolite structures  
(Bekkum et al., 1991)

The MFI - type (ZSM-5) zeolite is probably the most useful one. ZSM-5 zeolites with a wide range of  $\text{SiO}_2/\text{Al}_2\text{O}_3$  ratio can easily be synthesized. High siliceous ZSM-5 zeolites are more hydrophobic and hydro thermally stable compared with many other zeolites. Although the first synthetic ZSM-5 zeolite was discovered more than three decades ago (1972) new interesting applications are still emerging to this day. For example, its recent application in  $\text{NO}_x$  reduction, especially in the exhaust of lean-burned engine, has drawn much attention. Among various zeolite catalysts, ZSM-5 zeolite has the greatest number of industrial applications, covering from petrochemical production and refinery processing to environmental treatment.

### 3.2 Category of Zeolite

There are over 40 known natural zeolites and more than 150 synthetic zeolites have been reported (Meier, W.M. and Olson, D.H., 1992). The number of synthetic zeolites with new structure morphologies grows rapidly with time. Based on size of their pore opening, zeolites can be roughly divided into five major categories, namely 8-, 10-, and 12-member oxygen ring systems, dual pore systems and mesoporous systems (Wadlinger et al., 1967). Their pore structures can be characterized by crystallography, adsorption, measurements and/or through diagnostic reactions. One such diagnostic characterization test is the “constraint index” test. The concept of constraint index was defined as the ratio of the cracking rate constant of n-hexane to 3-methylpentane. The constraint index of a typical medium-pore zeolite usually ranges from 3 to 12 and those of the large-pore zeolites are the range 1-3. For materials with an open porous structure, such as amorphous silica alumina, their constraint indices are normally less than 1. On the index for erionite is 38.

A comprehensive bibliography of zeolite structures has been published by the International Zeolite Association (Meier, W.M. and Olson, D.H., 1992). The structural characteristics of assorted zeolites are summarized in Table 3.2

Zeolite with 10-membered oxygen rings normally possesses a high siliceous framework structure. They are of special interest in industrial applications. In fact, they were the first family of zeolite that was synthesized with organic ammonium salts. With pore openings close to the dimensions of many organic molecules, they are particularly useful in shape selective catalysis. The 10-membered oxygen ring zeolites also possess other important characteristic properties including high activity, high tolerance to coking and high hydrothermal stability. Among the family of 10-membered oxygen ring zeolites, the MFI - type (ZSM-5) zeolite as presented in Figure 3.3 is probably the most useful one. ZSM-5 zeolite has two types of channel systems of similar sized, one with a straight channel of pore opening  $5.3 \times 5.6 \text{ \AA}$  and the other with a tortuous channel of pore opening  $5.1 \times 5.5 \text{ \AA}$ . Those intersecting channels are perpendicular to each other, generating a three dimensional framework. ZSM-5 zeolites with a wide range of  $\text{SiO}_2/\text{Al}_2\text{O}_3$  ratio can easily be synthesized. High

siliceous ZSM-5 zeolites are more hydrophobic and hydro thermally stable compared with many other zeolites. Although the first synthetic ZSM-5 zeolite was discovered more than two decades ago (1972) new interesting applications are still emerging to this day. For example, its recent application in NO<sub>x</sub> reduction, especially in the exhaust of lean-burned engine, has drawn much attention. Among various zeolite catalysts, ZSM-5 zeolite has the greatest number of industrial applications, covering from petrochemical production and refinery processing to environmental treatment.

**Table 3.2** Structural characteristics of selected zeolites (Meier, W.M. and Olson, D.H., 1992).

Zeolite	Number of rings	Pore opening Å	Pore/Channel structure	Void volume (ml/g)	D <sub>Frame</sub> <sup>a</sup> (g/ml)	CI <sup>b</sup>
<i>8-membered oxygen ring</i>						
Erionite	8	3.6x5.1	Intersecting	0.35	1.51	38
<i>10-membered oxygen ring</i>						
ZSM-5	10	5.3x5.6 5.1x5.5	Intersecting	0.29	1.79	8.3
ZSM-11	10	5.3x5.4	Intersecting	0.29	1.79	8.7
ZSM-23	10	4.5x5.2	One-dimensional	-	-	9.1
<i>Dual pore system</i>						
Ferrierite (ZSM-35, FU-9)	10,8	4.2x5.4 3.5x4.8	One-dimensional 10:8 intersecting	0.28	1.76	4.5
MCM-22	12	7.1	Capped by 6 rings	-	-	1-3
Mordenite	10	Elliptical				
	12	6.5x7.0	One-dimensional	0.28	1.70	0.5
	8	2.6x5.7	12:8 intersecting			
Omega (ZSM-4)	12	7.4	One-dimensional	-	-	2.3
	8	3.4x5.6	One-dimensional	-	-	0.6
<i>12membered oxygen ring</i>						
ZSM-12	12	5.5x5.9	One-dimensional	-	-	2.3
Beta	12	7.6x6.4 5.5x5.5	Intersecting	-	-	0.6
Faujasite (X,Y)	12	7.4	Intersecting	0.48	1.27	0.4
	12	7.4x6.5	12:12 intersecting			
<i>Mesoporous system</i>						
VPI-5	18	12.1	One-dimensional	-	-	-
MCM41-S	-	16-100	One-dimensional	-	-	-

<sup>a</sup>Framework density

<sup>b</sup>Constraint index



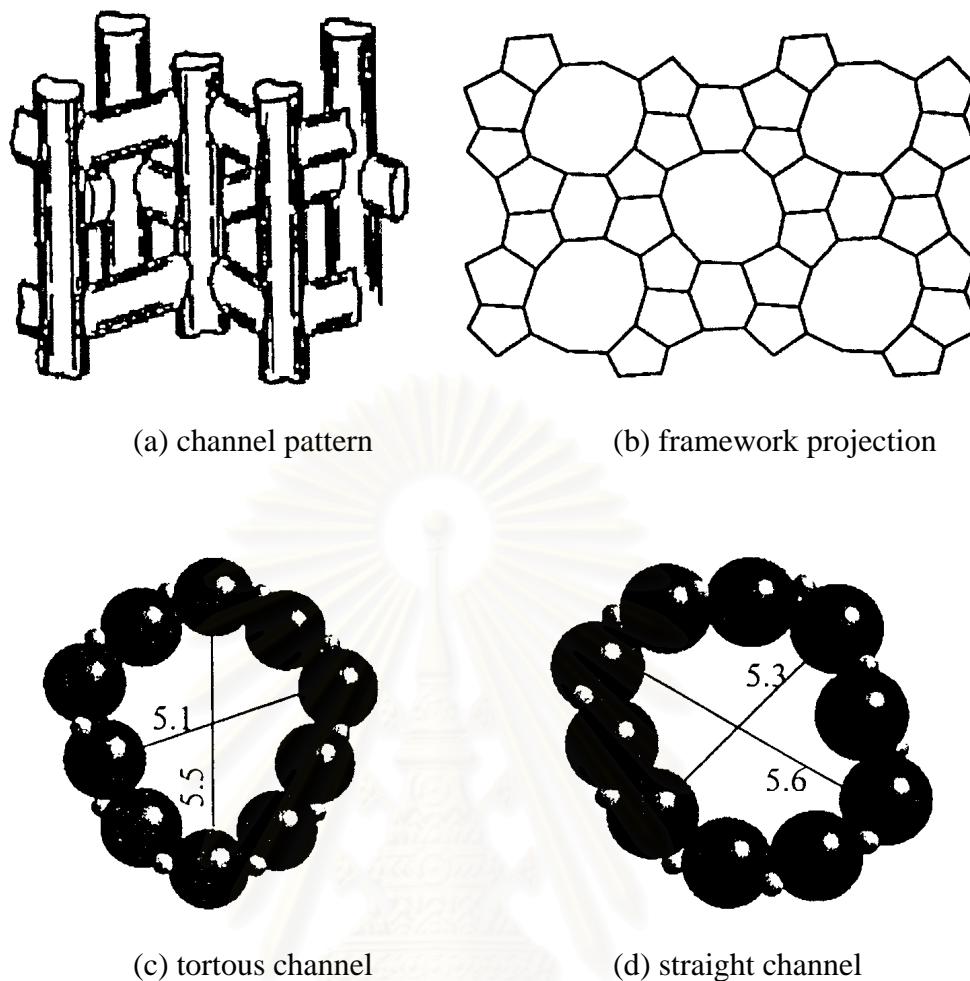


**Figure 3.3** Structure of ZSM-5 (Meier, W.M. and Olson, D.H., 1992).

Although the 10-membered oxygen ring zeolite was found to possess remarkable shape selectivity, catalysis of large molecules may require a zeolite catalyst with a large-pored opening. Typical 12-membered oxygen ring zeolites, such as faujasite-type zeolites, normally have pore opening greater than 5.5 Å and hence are more useful in catalytic applications with large molecules, for example in trimethylbenzene (TMB) conversions. Faujasite (X or Y; Figure 3.4 (Meier, W.M. and Olson, D.H., 1992) ) zeolites can be synthesized using inorganic salts and have been widely used in catalytic cracking since 1960s. The framework structures of beta zeolite and ZSM-12 are shown in Figure 3.5 and 3.6 , respectively.

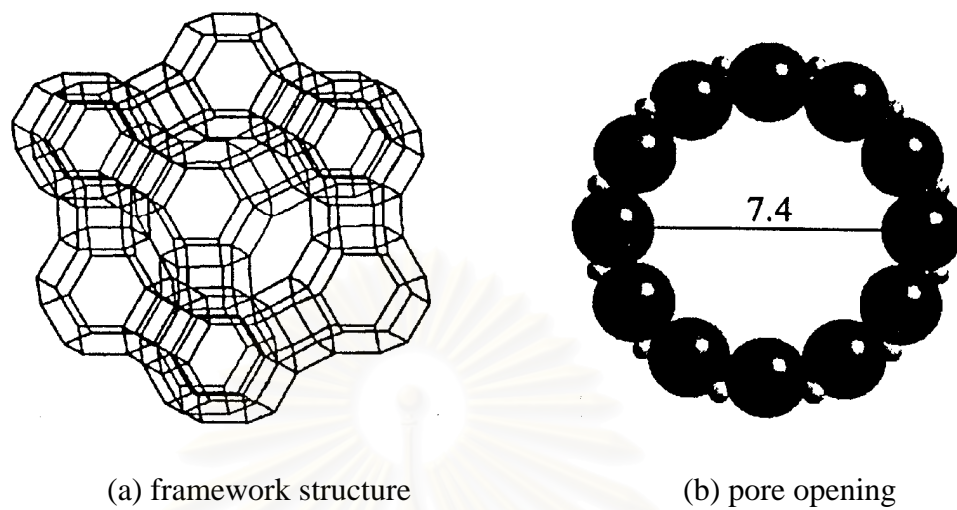


**Figure 3.4** Structure of Faujasite (Meier, W.M. and Olson, D.H., 1992).

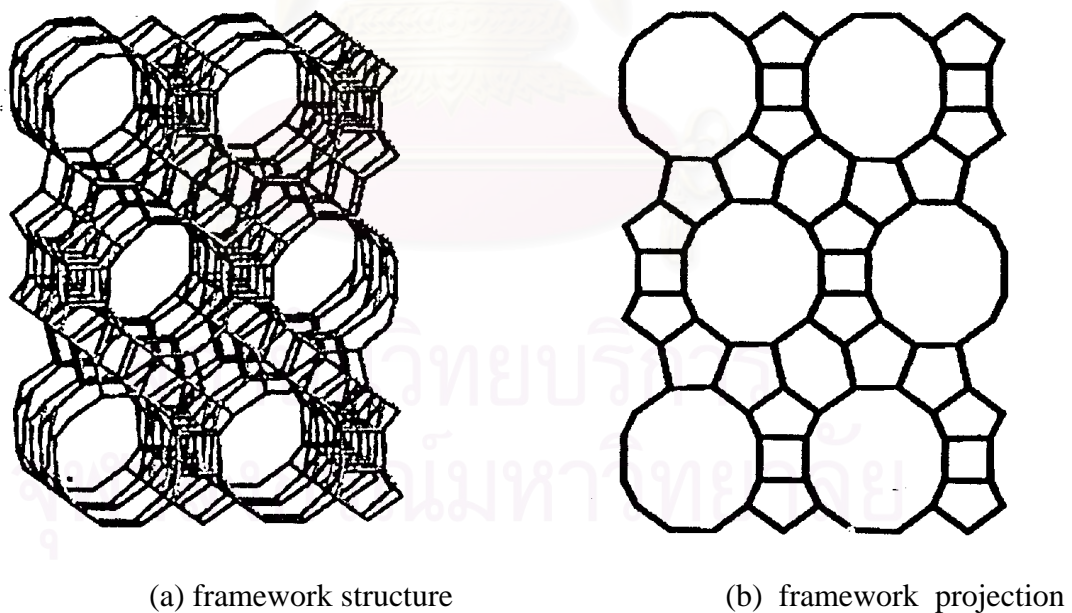


**Figure 3.5** Structure of beta zeolite (Meier, W.M. and Olson, D.H., 1992).

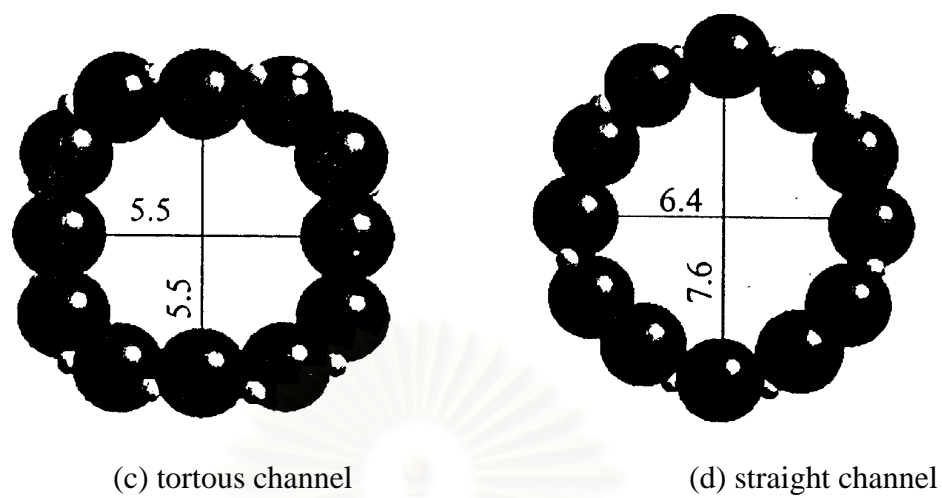


**Figure 3.5** Structure of beta zeolite (Meier, W.M. and Olson, D.H., 1992).

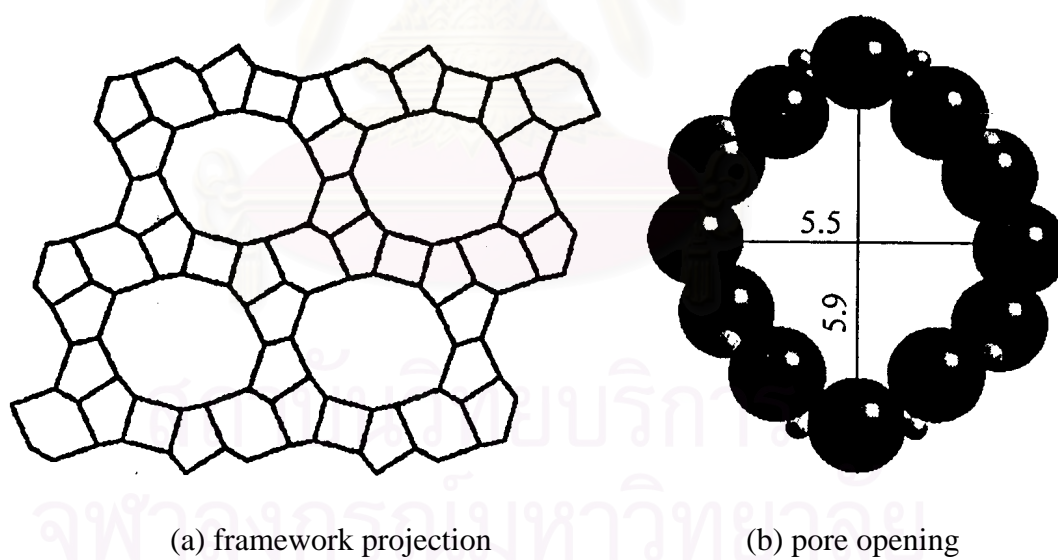


**Figure 3.6** Structure of zeolite ZSM-12 (Meier, W.M. and Olson, D.H., 1992).

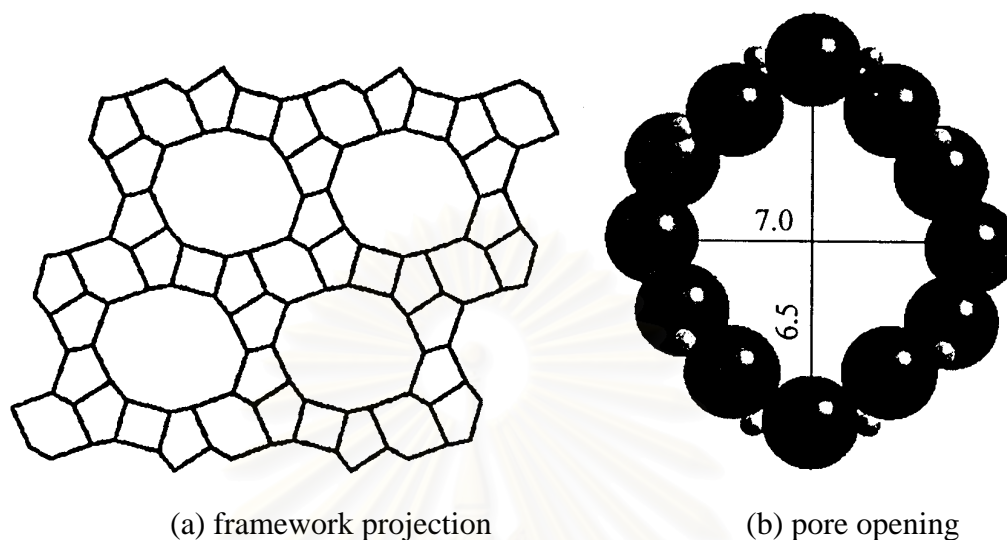


**Figure 3.7** Structure of Mordenite (Meier, W.M. and Olson, D.H., 1992).

Zeolites with a dual pore system normally possess interconnecting pore channels with two different pore opening sizes. Mordenite is a well-known dual pore zeolite having a 12-membered oxygen ring channel with pore opening  $6.5 \times 6.7 \text{ \AA}$  which is interconnected to 8-membered oxygen ring channel with opening  $2.6 \times 5.7 \text{ \AA}$  (Figure 3.7 (Chen et al., 1999)). MCM-22, which was found more than 10 years ago, also possesses a dual pore system. Unlike Mordenite, MCM-22 consists of 10- and 12-membered oxygen rings (Figure 3.8 (Meier, W.M. and Olson, D.H., 1992)) and thus shows prominent potential in future applications.

In the past decade, many research efforts in synthetic chemistry have been invested in the discovery of large-pored zeolite with pore diameter greater than 12-membered oxygen rings. The recent discovery of mesoporous materials with controllable pore opening (from 12 to more than  $100 \text{ \AA}$ ) such as VPI-5, MCM-41S undoubtedly will shed new light on future catalyst applications.

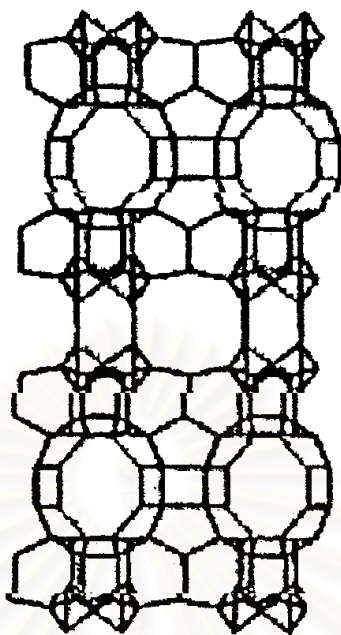


**Figure 3.8** Framework structure of MCM-22 (Meier, W.M. and Olson, D.H., 1992).

### 3.3 Zeolite Active sites

#### 3.3.1 Acid sites

Classical Brønsted and Lewis acid models of acidity have been used to classify the active sites on zeolites. Brønsted acidity is proton donor acidity; a tridiagonally coordinated alumina atom is an electron deficient and can accept an electron pair, therefore behaves as a Lewis acid (Barthoment, D., 1984 and Ashton et al., 1985).

In general, the increase in Si/Al ratio will increase acidic strength and thermal stability of zeolite (Sano et al., 1987). Since the numbers of acidic OH groups depend on the number of aluminium in zeolites framework, decrease in Al content is expected to reduce catalytic activity of zeolite. If the effect of increase in the acidic centers, increase in Al content, shall result in enhancement of catalytic activity

Based on electrostatic consideration, the charge density at a cation site increase with increase Si/Al ratio. It was conceived that these phenomena are related to reduction of electrostatic interaction between framework sites, and possibly to

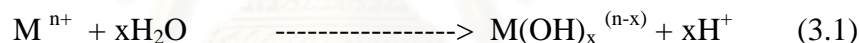
difference in the order of aluminum in zeolite crystal-the location of Al in crystal structure (Ashton et al., 1985).

An improvement in thermal or hydrothermal stability has been ascribed to the lower density of hydroxyl groups, which is parallel to that of Al content (Barthomont, D., 1984). A longer distance between hydroxyl groups decrease the probability of dehydroxylation that generates defects on structure of zeolites.

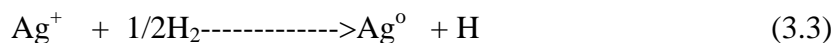
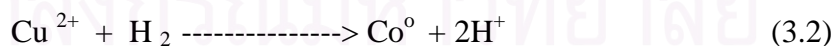
### 3.3.2 Generation of Acid Centers

Protonic acid centers of zeolite are generated in various ways. Figure 3.9 depicts the thermal decomposition of ammonium-exchanged zeolite yielding the hydrogen form (Satterfield, C.N, 1991).

The Brønsted acidity due to water ionization on polyvalent cations, described below, is depicted in Figure 3.10 (Tanake et al., 1989).



The exchange of monovalent ions by polyvalent cations could improve the catalytic property. Those highly charged cations create very centers by hydrolysis phenomena. Brønsted acid sites are also generated by the reduction of transition metal cations. The concentration of OH groups of zeolite containing transition metals was noted to increase by hydrogen at 2.5 – 450 °C to increase with the rise of the reduction temperature (King, R. B., 1994).



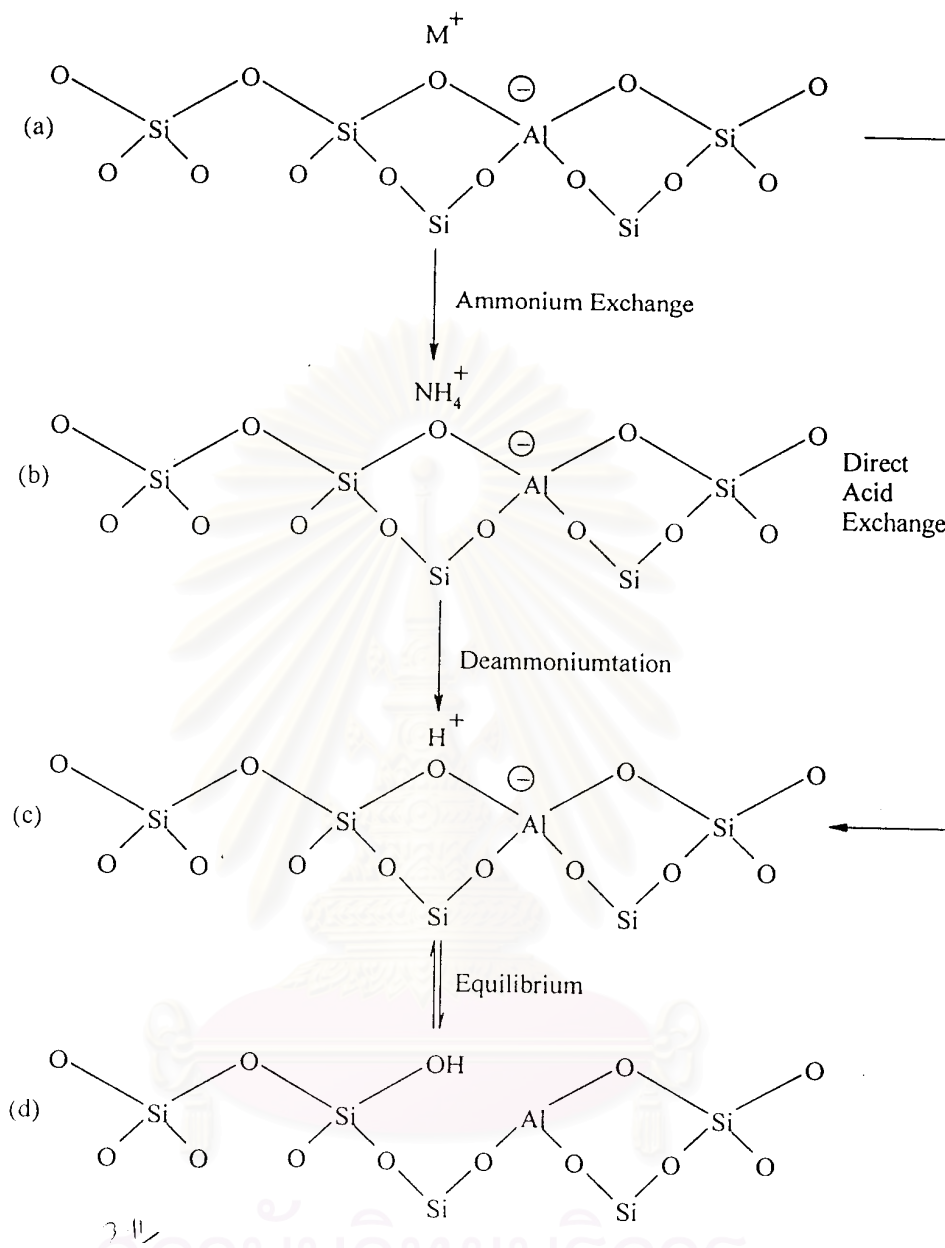


**Figure 3.9** Diagram of the surface of a zeolite framework (Szoztak, R., 1989).

- In the as-synthesis form  $M^+$  either an organic cation or an alkali metal cation.
- Ammonium in exchange produces the  $NH_4^+$  exchanged form.
- Thermal treatment is used to remove ammonia, producing the  $H^+$ , acid form.
- The acid form in (c) is in equilibrium with the shown in (d), where is a silanol group adjacent to tricoordinate aluminium.

The formation of Lewis acidity from Brønsted acid sites is depicted in Figure 3.11 [59]. The dehydration reaction decrease the number of protons and increases that of Lewis sites. Brønsted (OH ) and Lewis (-Al-) sites can be present simultaneously in the structure of zeolite at high temperature. Dehydroxylation is thought to occur in ZSM-5 zeolite above at 500 °C and calcination at 800 to 900 °C produces irreversible dehydroxylation, which causes defection in crystal structure of zeolite.

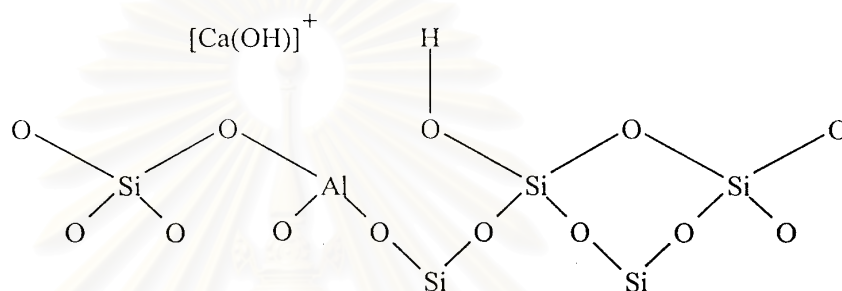


**Figure 3.10** Water molecules co-ordinated to polyvalent cation are dissociated by heat treatment yielding Brønsted acidity [59].

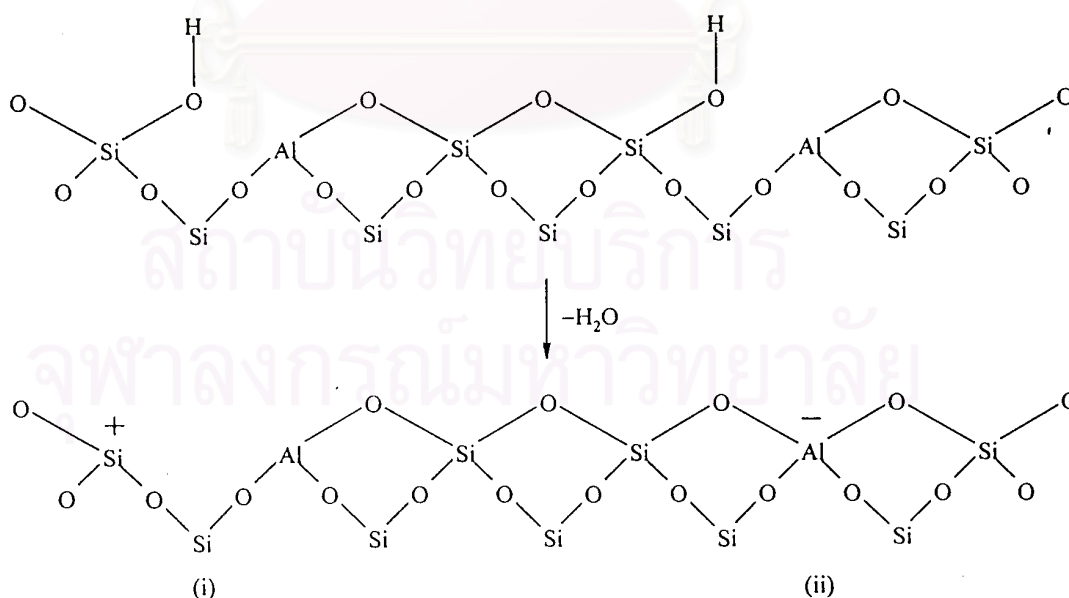


**Figure 3.11** Lewis acid site developed by dehydroxylation of Brønsted acid site [59].



Dealumination is believed to occur during dehydroxylation, which may result from the steam generation within the sample. The dealumination is indicated by an increase in the surface concentration of aluminum on the crystal. The dealumination process is expressed in Figure 3.12 (Tanake et al., 1989). The extent of dealumination monotonously increases with the partial pressure of steam.

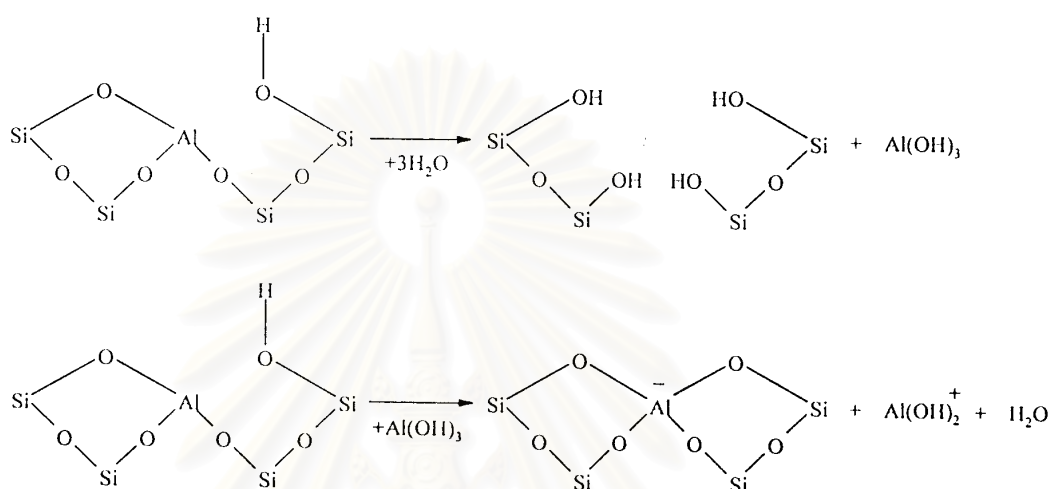


**Figure 3.12** Steam dealumination process in zeolite (Tanake et al., 1989).

The enhancement of the acid strength of OH groups is recently proposed to be pertinent to their interaction with those aluminum species sites tentatively expressed in Figure 3.13 (Tanake et al., 1989). Partial dealumination might therefore yield a catalyst of higher activity while severe steaming reduces the catalytic activity.

### 3.3.3 Basic Sites

In certain instances reactions have been shown to be catalyzed at basic (cation) site in zeolite without any influences from acid sites. The best-characterized example of this is that K-Y which splits n-hexane isomers at  $500^\circ\text{C}$ . The potassium cation has been shown to control the unimolecular cracking ( $\beta$ -scission). Free radical mechanisms also contribute to surface catalytic reactions in these studies.

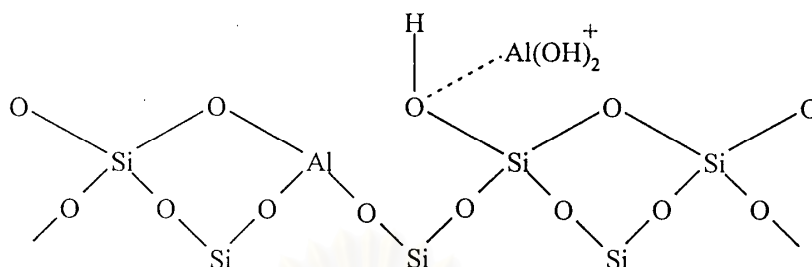


**Figure 3.13** The enhancement of the acid strength of OH groups by their interaction with dislodged aluminum species (Tanake et al., 1989).

### 3.4 Shape Selective

Many reactions involving carbonium intermediates are catalyzed by acidic zeolite. With respects to a chemical standpoint the reaction mechanisms are not fundamentally different with zeolites or with any the acidic oxides. What zeolite add is shape selectivity effect. The shape selective characteristics of zeolites influence their catalytic phenomena by three modes: shape selectivity, reactants shape selectivity, products shape selectivity and transition states shape selectivity. These types of selectivity are illustrated in Figure 3.14.

Reactants of charge selectivity results from the limited diffusibility of some of the reactants, which cannot effectively enter and diffuse inside crystal pore structures of the zeolites. Product shape selectivity occurs as slowly diffusing product molecules cannot escape from the crystal and undergo secondary reaction. This reaction path is established by monitoring changes in product distribution as a function of varying contact time.

Restricted transition state shape selectivity is a kinetic effect from local environment around the active site, the rate constant for a certain reaction mechanism is reduced of the space required for formation of necessary transition state is restricted.

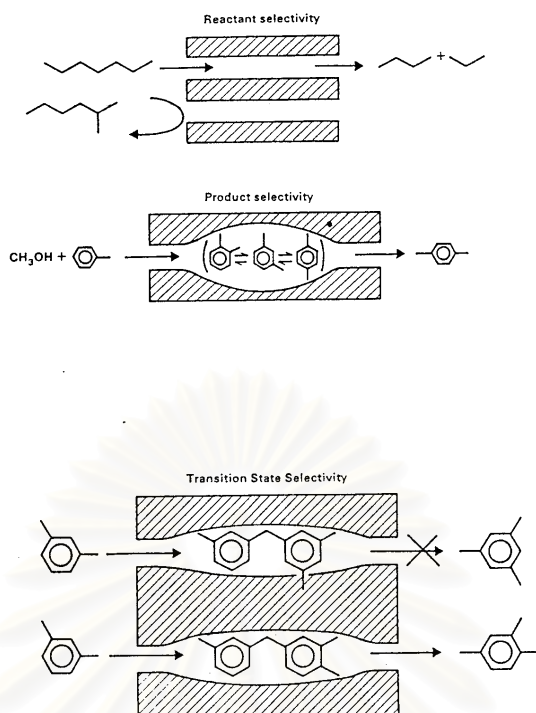


**Figure 3.14** Diagram depicting the three type of selectivity (Szoztak, R.,1989).

The critical diameter (as opposed to the length) of the molecules and the pore channel diameter of zeolites are important in predicting shape selective effects. However, molecules are deformable and can pass through opening, which are smaller than their critical diameters. Hence, not only size but also the dynamics and structure of the molecules must be taken into account.

### 3.5 Zeolite Synthesis

Zeolites are generally synthesized by a hydrothermal process from a source of alumina (e.g., sodium aluminate or aluminium sulfate) and of silica (e.g., a silica sol, fumed silica, or sodium water glass) and an alkali such as NaOH, and/or a quaternary ammonium compound. An inhomogeneous gel is produced which gradually crystallizes, in some cases forming more than one type of zeolite in succession. Nucleation effects can be important, and an initial induction period at near ambient temperature may be followed by crystallization temperature that may range up to 200 °C or higher. The pressure is equal to the saturated vapor pressure of the water present.

The final product depends on a complex interplay between many variables including  $\text{SiO}_2/\text{Al}_2\text{O}_3$  ratio in the starting medium, nucleating agents, temperature, pH, water content, aging, stirring, and the presence of various inorganic and organic cations. Much remains to be learned about how the initial reaction mixture forms the precursor species and how these arrange into the final crystalline products. A key concept is that the cations present give rise to a templating action, but clearly the process is more complex.

Bauer and coworkers in the early 1960s developed the use of reaction mixtures containing quaternary ammonium ions or other or other cations to direct the crystallization process. In their work and succeeding studies, a primary motivation was to attempt to synthesize zeolites with large apertures than X and Y. This did not occur, but instead organic species were found to modify the synthesis process in a variety of ways that led to the discovery of many new zeolites, and new methods of synthesizing zeolite with structures similar to previously know zeolite.

The mechanism of action of the organic species is still controversial. It was originally thought to be primarily a templating effect, but later it was found that at least some of zeolites could be synthesized without an organic template. Further, organic species other than quaternary ammonium compounds had directing effects not readily ascribed to their size or shape. However, an important result was the zeolites of higher  $\text{SiO}_2/\text{Al}_2\text{O}_3$  ratio than before could be synthesized. Previously, only structures with  $\text{SiO}_2/\text{Al}_2\text{O}_3$  ratios of about 10 or less could be directly forms, but with organic additives, zeolites with ratio of 20 to 100 or more can be directly prepared.

After synthesis the zeolite are washed, dried, heated to remove water of crystallization, and calcined in air, e.g., at about  $550^\circ\text{C}$ . Organic species are also thus removed. For most catalytic purpose, the zeolite is converted into acidic form. For some zeolites this can be achieved by treatment with aqueous HCl without significantly altering the framework structure. For other zeolites  $\text{Na}^+$  is replaced with  $\text{NH}_4^+$  via an ammonium compound such as  $\text{NH}_4\text{OH}$ ,  $\text{NH}_4\text{Cl}$  or  $\text{NH}_4\text{NO}_3$ . Upon heating  $\text{NH}_3$  is driven off, leaving the zeolite in the acid form. For some reaction a

hydrogenation component such as platinum or nickel is introduced by impregnation or ion exchange (Satterfield, C.N., 1991).

### 3.6 Aromatics

Aromatics ( $C_nH_{2n-6}$ ) are similar to naphthenes, but they contain a stabilized unsaturated ring core. Example of aromatics are benzene, toluene and aniline. Typical aromatics are show in figure 3.15.

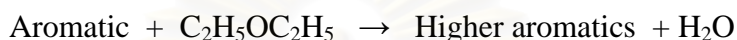
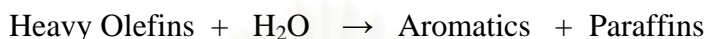
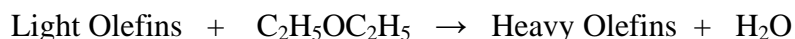


**Figure 3.15** Aromatics (Sadeghbeigi, R, 2000).

Aromatics are compounds that contain at least one benzene ring. The benzene is very stable and do not crack to smaller componenrs. Aromatics are not preferable as FCC feedstock because most of the molecules will not crack. The cracking of aromatics mainly involves breaking off the side chains, and this can result in excess fuel gas yield. In addition, some of the aromatic compounds contain several rings (polynuclear aromatics) that can “compact” to form what is commonly called “chicken wire”. Some of these compacted aromatics will end up on the catalyst as carbon residue (coke), and some will become slurry product. In comparison to paraffins, the cracking of aromatic stocks results in lower conversion, lower gasoline yield, and less liquid volume gain with higher gasoline octane (Sadeghbeigi, R, 2000).

### 3.7 Reaction Mechanism of Ethanol to Aromatics

The reaction of ethanol to hydrocarbon products is vigorously exothermic, with a theoretical adiabatic temperature rise of about 600 °C. The reaction path is believed to pass through a number of series and parallel steps. The mechanism is complex and is discussed elsewhere. A simplified path is given below (Chang,C. D.,1983 and Iordache, et al.,1988).



The first step in the reaction sequence is the dehydration of ethanol to an equilibrium mixture of diethylether (DEE), ethanol and water. The DEE then reacts further to form a mixture of light olefins. As the concentration of DEE is depleted, the equilibrium of reaction is disturbed and further dehydration of ethanol take place. The DEE alkylates the light olefins (mostly propylene and butanes) to high olefins, which can then further react with one another to form aromatics and paraffins. If any residual DEE remains at the point where aromatics form, those aromatics are readily alkylated to higher carbon number of C<sub>10</sub>. The heaviest component is durene (1,2,4,5-tetraethylbenzene), which lies near the high end of the gasoline boiling range. No components with normal boiling points above the gasoline boiling range are produced.

The early work of Chang showed that, high temperature favours selectivity to light olefins. Mobil found that by combining the factors of reduced catalyst activity with high operating temperatures, it was possible to switch the Ethanol to Gasoline (ETG) selectivity towards an olefin rich spectrum. This route was named the Ethanol to Olefins (ETO) process, and gives a product that is rich in propylene and butenes together with a good aromatic rich C<sub>5+</sub> gasoline fraction.

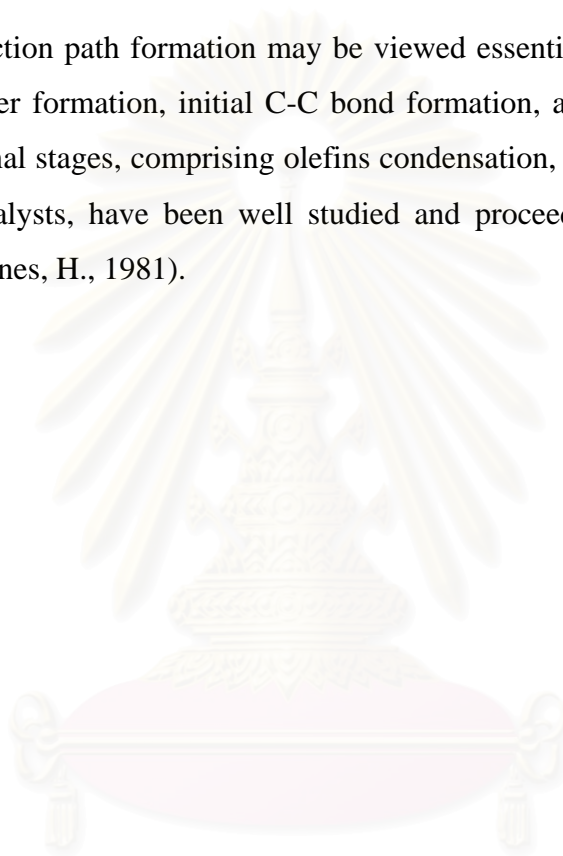
Voltz and Wise has proposed scheme A to contain a direct path to olefins from ethanol:



OLEFINS

Scheme A

The reaction path formation may be viewed essentially as composed of three key steps – ether formation, initial C-C bond formation, and aromatization with H-transfer. The final stages, comprising olefins condensation, cyclization and H-transfer over acidic catalysts, have been well studied and proceed via classical carbenium mechanisms (Pines, H., 1981).



สถาบันวิทยบริการ  
จุฬาลงกรณ์มหาวิทยาลัย

## CHAPTER IV

### EXPERIMENTAL

#### 4.1 Catalyst Preparation

In this study, five of MFI zeolite catalysts, having different particle size but the same Si/Al ratio ( $\text{Si/Al} \approx 40$ ) and MFI commercial catalyst were also used. Ga/MFI was prepared for ethanol aromatization. The preparation of Ga/MFI was described as follows:

##### 4.1.1 Chemicals

The details of chemicals used in the preparation procedure of MFI zeolite were shown in Table 4.1

**Table 4.1** The chemicals used in the catalyst preparation

Chemical	Supplier
-Tetraethylammonium hydroxide [TEAOH] (40% by weight aqueous solution)	Fluka
-Cataloid as a source of $\text{SiO}_2$ (30% by weight aqueous solution)	Form Japan
-Sodium hydroxide [NaOH]	Merck
-Aluminium chloride [ $\text{AlCl}_3$ ]	Aldrich
-Gallium(III) nitrate hydrate [ $\text{Ga}(\text{NO}_3)_3$ ]	Aldrich

##### 4.1.2 Preparation of NaZSM-5 ( MFI )

The preparation procedure of MFI by rapid crystallization method was shown in Figure 4.1, while reagents were shown in table 4.2. This method can



advantageously and rapidly prepare the uniform and fine zeolite crystals with the following improvements: (i) the preparation of supernatant liquid was separated from that of gel, which was important to prepare the uniform crystals, (ii) the precipitated gel was milled before the hydrothermal treatment, which was essential to obtain the uniform and fine crystals, and (iii) the temperature under the hydrothermal treatment was programmed to minimize the time which was necessary for the crystallization. The detail preparation procedures of MFI were described below.

**Table 4.2** Reagents used for the preparation of Na/MFI: Si/Al = 40

Solution for the gel preparation	Solution for the decant-solution preparation
<p><u>Solution A1</u></p> <p>AlCl<sub>3</sub> 1.125 g</p> <p>TPABr 5.72 g</p> <p>NaCl 11.95 g</p> <p>De-ionized water 60 ml</p> <p>H<sub>2</sub>SO<sub>4</sub> 3.4 ml</p>	<p><u>Solution A2</u></p> <p>AlCl<sub>3</sub> 1.125 g</p> <p>TPABr 7.53 g</p> <p>De-ionized water 60 ml</p> <p>H<sub>2</sub>SO<sub>4</sub> 3.4 ml</p>
<p><u>Solution B1</u></p> <p>De-ionized water 45 ml</p> <p>Sodium silicate 69 g</p>	<p><u>Solution B2</u></p> <p>De-ionized water 45 ml</p> <p>Sodium silicate 69 g</p>
<p><u>Solution C1</u></p> <p>TPABr 2.16 g</p> <p>NaCl 40.59 g</p> <p>NaOH 2.39 g</p> <p>De-ionized water 208 ml</p> <p>H<sub>2</sub>SO<sub>4</sub> 1.55 ml</p>	<p><u>Solution C3</u></p> <p>NaCl 26.27 g</p> <p>De-ionized water 45 ml</p>

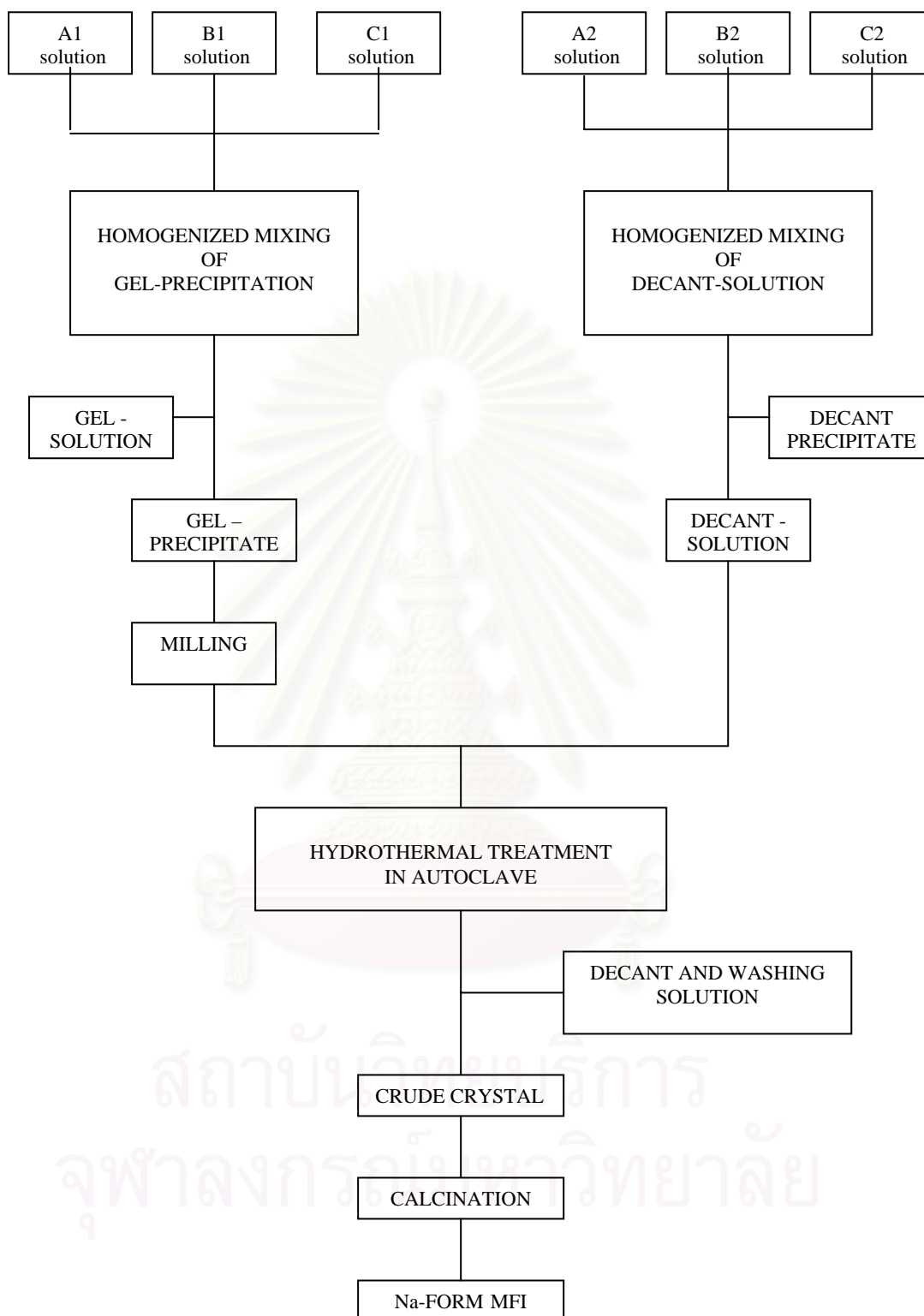


**Figure 4.1** The preparation procedure of MFI by rapid crystallization method.

#### 4.1.2.1 Preparation of Gel Precipitation and Decantation Solution

A supernatant liquid was separated from the gel, which was important for preparing the uniform crystals. A gel mixture was prepared by adding solution A-1 and solution B-1 into solution C-1 drop wise with vigorous stirring using a magnetic stirrer at room temperature. The pH of the mixed solution was maintained within the range 9-11 because it was expected that this pH range was suitable for precipitation. The gel mixture was separated from the supernatant liquid by a centrifuge. The precipitated gel mixture was milled for 1 h by a powder miller (Yamato-Notto, UT-22). The milling procedure was as follows: milled 15 min → centrifuge (to remove the liquid out) → milled 15 min → centrifuge → milled 15 min. Milling the gel mixture before the hydrothermal treatment was essential to obtain the uniform, fine crystals.

A decantation solution was prepared by adding solution A-2 and solution B-2 into solution C-2 same as for the preparation of the gel mixture. During the time the supernatant liquid from A-2, B-2, and C-2 is mixing together. The pH of the solution was adjusted to between 9-11.  $\text{H}_2\text{SO}_4$  (conc.) or 1 M NaOH solution were used to adjust pH of the decant mixture to an appropriate level if it is necessary. The colorless supernatant liquid was separated from the mixture by sedimentation and centrifugation.

#### 4.1.2.2 Crystallization

The mixture of the milling precipitate and the supernatant of decant solution was charged in a 500 ml Pyrex glass container. The glass container was placed in a stainless steel autoclave. The atmosphere in the autoclave was replaced by nitrogen gas and pressurized up to 3  $\text{kg}/\text{cm}^2$  gauge. In order to vary the particle sizes of MFI, the mixture in the autoclave was heated from room temperature to 160°C with various heating rates 0.4, 0.5, 0.9, 1.0, and 1.5 °C/min, and then up to 210 °C with a constant heating rate of 12 °C/h while being stirred at 60 rpm, followed by cooling of the hot mixture to room temperature in the autoclave overnight. The temperature was programmed to minimize the time necessary for the crystallization. The product crystals were washed with de-ionized water about 8 times using the centrifugal

separator (about 15-20 min. for each time), to remove  $\text{Cl}^-$  from the crystals, and dried in an oven at  $110\text{ }^\circ\text{C}$  for at least 3 h.

#### 4.1.2.3 Calcination

The dry crystals were calcined in an air stream at  $540\text{ }^\circ\text{C}$  for 3.5 h, by heating them from room temperature to  $540\text{ }^\circ\text{C}$  in 1 h, to burn off the organic template and leave the cavities and channels in the crystals. The calcined crystals were finally cooled to room temperature in a desiccator. The obtained Na/MFI was the parent MFI zeolite which was further transformed to the other appropriate forms for the experiments in this study.

Moreover, the Na/MFI obtained from each batch was checked by using the X-Ray Diffraction (XRD) analysis to confirm the MFI structure and crystallinity of sample. If, unfortunately, the XRD pattern could not be acceptable, the sample would be discarded and a new sample has to be made.

#### 4.1.2.4 Ammonium ion-exchange

To make  $\text{NH}_4$ -ZSM-5, the parent Na/ MFI powder was firstly mixed with 1 M  $\text{NH}_4\text{NO}_3$  solution at 30 ml per gram of catalyst. In the procedure, the catalyst amounts did not exceed 5 grams to approach complete exchange. The slurry of zeolite and solution was then stirred and heated on a hot plate, maintained at  $80\text{ }^\circ\text{C}$  by reflux. After heating the mixture for about 1 h, the mixture was cooled down to room temperature and centrifuged to remove the used solution. The remained crystals were mixed again with  $\text{NH}_4\text{NO}_3$  solution in the same amount. The previous step was repeated. The exchanged catalyst was then washed twice with deionized water by using a centrifugal separator. Then, the ion exchange crystal was dried at  $110\text{ }^\circ\text{C}$  for at least 3 h. in oven. The dried catalyst was obtained the  $\text{NH}_4$ -form of MFI. The  $\text{NH}_4$ / MFI was converted to H-form MFI by removing  $\text{NH}_3$  species from the catalyst surface.  $\text{NH}_3$  can be removed by thermal treatment of the  $\text{NH}_4$ / MFI zeolite. This was done by heating a sample in a furnace from ambient temperature to  $540\text{ }^\circ\text{C}$  in 1 h and holding the sample at  $540\text{ }^\circ\text{C}$  for 3.5 h. After this step, the obtained crystals were H-zeolite.

### 4.1.3 Gallium loading by ion-exchanged

The suitable metal-exchanged technique contacting the zeolite with a solution which contains the salt of the desired replacing cation. A preferred exchange solution is gallium nitrate. Approximately 3 g. of catalyst was stirred with 150 ml of a dilute (0.01 M) gallium nitrate solution. The metal exchange was typically carried out at 80 °C for 24 h. More repeats of ion-exchanged step were required upon the amount of gallium needed. The wet cake obtain by separation from the solution was washed with de-ionized water and dried at 110 °C overnight. Finally, dry crystal was heated in air with the constant heating rate of 10 °C/min up to 350 °C and maintain for 3.5 h.

### 4.2 Pretreatment condition

The pretreatment procedure used in this study concerns the hydrothermal treatment condition. The catalysts were pretreated in He while elevating the temperature from room temperature to 800 °C with heat rate 10 °C/min. The catalyst samples were then kept at 800 °C for 24 h while adding 10% mole of water vapor. The catalysts were then cooled down to room temperature in the He stream.

### 4.3 Characterization

#### 4.3.1 X- Ray Diffraction analysis (XRD)

Crystallinity and X-ray diffraction (XRD) patterns of the catalysts were performed by a X-ray diffractometer SEIMENS D500 connected with a personal computer with Diffract AT version 3.3 program for fully control of the XRD analyzer. The experiments were carried out by using  $\text{CuK}\alpha$  radiations with Ni filter and the operating condition of measurement are shown as follows:

2 $\theta$  range of detection : 4 – 40 °  
Resolution : 0.04 °  
Number of Scan : 10

The functions of based line subtraction and smoothing were used in order to get the well formed XRD spectra.

#### **4.3.2 X-Ray Fluorescence analysis (XRF)**

Quantities of  $\text{SiO}_2/\text{Al}_2\text{O}_3$  in the sample were determined by atomic absorption spectroscopy using Varian, Spectra A8000 at the Department of Science Service, Ministry of Science Technology and Environment.

#### **4.3.3 BET surface area measurement**

The surface area ( $A_{\text{BET}}$ ) of the samples was calculated using BET technique, Micromeritics ASAP 2020.

#### **4.3.4 Scanning Electron Microscopy (SEM)**

Scanning Electron Microscopy was employed for including the shape and size of the prepared zeolite crystal. The JEOL JSM-35 CF model at the Scientific and Technological Research Equipment Centre, Chulalongkorn University (STREC) was used for this purpose

#### **4.3.5 $^{27}\text{Al}$ Magnetic Angle Spinning Nuclear Magnetic Resonance ( $^{27}\text{Al}$ MAS NMR)**

Quantitative analysis of aluminum tetrahedral in zeolite was conformed by  $^{27}\text{Al}$  Magnetic Angle Spinning Nuclear Magnetic Resonance ( $^{27}\text{Al}$  MAS NMR, BRUKER DPX-300 spectroscopy operating at 78.2 MHz) at National Metal and Materials Technology Center (MTEC) Bangkok.

#### 4.3.6 Temperature Programmed Adsorptions of Ammonia (NH<sub>3</sub>-TPD)

The acid properties were observed by Temperature programmed desorption (TPD) equipment by using micromeritics chemisorb 2750 Pulse Chemisorption System.

### 4.4 Reaction Testing

#### 4.4.1 Chemicals and Reagents

Ethanol was available from MERCK, 99.9 % for ethanol aromatization.

#### 4.4.2 Instruments and Apparatus

(a) Reactor: The reactor was a conventional micro reactor made from a quartz tube with 6 mm inside diameter. The reaction was carried out under N<sub>2</sub> gas flow and atmospheric pressure.

(b) Automatic Temperature Controller: This consists of a magnetic switch connected to a variable voltage transformer and a RKC temperature controller connected to a thermocouple attached to the catalyst bed in reactor. A dial setting established a set point at any temperatures within the range between 0°C to 600°C.

(c) Electric Furnace: This supply the required heated to the reactor for reaction. The reactor could be operated from room temperature up to 600° C at maximum voltage of 220 volt.

(d) Gas Controlling Systems: Nitrogen was equipped with pressure regulator (0-120 psig), an on-off valve and a needle valve were used to adjust flow rate of gas.

(e) Gas Chromatographs: Operating conditions were shown in Table 4.3.

**Table 4.3** Operating condition for gas chromatograph

Gas chromatograph	Shimadzu GC8A	Shimadzu GC14B	Shimadzu GC14B
Detector	TCD	FID	FID
Column	Porapack-Q	VZ-10	Bentone 34
Carrier gas	He (99.999%)	N <sub>2</sub> (99.999%)	N <sub>2</sub> (99.999%)
Carrier gas flow	30 ml./min.	30 ml./min.	30 ml./min
Column temperature	90°C	70°C	100°C
Detector temperature	100°C	140°C	200°C
Injector temperature	100°C	100°C	200°C
Analyzed gas	Ethanol	Hydrocarbon C <sub>1</sub> -C <sub>4</sub>	Hydrocarbon

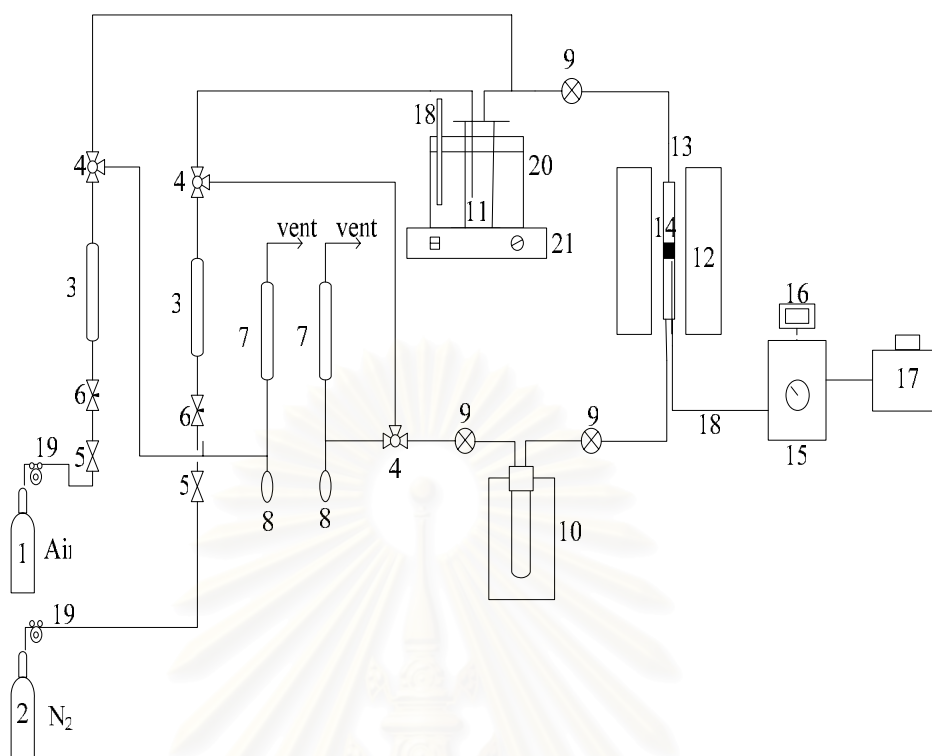
สถาบันวิทยบริการ  
จุฬาลงกรณ์มหาวิทยาลัย



#### 4.4.3 Reaction Method

The ethanol conversion was carried out by using a conventional flow as shown in Figure 4.2. A 0.1 portion of the catalyst was packed in the quartz tubular reactor. The reaction was carried out under the following procedure:

- 1) Adjust the pressure of nitrogen to  $1 \text{ kg/cm}^2$ , and allow the gas to flow through a Rota meter, measure the outlet gas flow rate by using a bubble flow meter.
- 2) Heat up the reactor (under  $\text{N}_2$  flow) by raising the temperature from room temperature to  $450^\circ \text{C}$  in 45 min and then hold at this temperature about 30 min for preheating catalyst.
- 3) Put ethanol 20 ml in saturator and set the temperature of water bath at  $25^\circ \text{C}$ . At this temperature, the concentrations of ethanol in saturator were 20% mol.
- 4) Start to run the reaction by adjusting the two three way valves to allow nitrogen gas to pass through reactants inside saturator in water bath.
- 5) Take sample for analyzed by gas chromatograph after the reaction ran for 1 h.



- |                                     |                                   |
|-------------------------------------|-----------------------------------|
| 1. Air cylinder                     | 2. Ar cylinder                    |
| 3. Mass flow controller             | 4. Three-way-valve                |
| 5. Ball valve                       | 6. Needle valve                   |
| 7. Rotary meter                     | 8. Rubber cock                    |
| 9. Sampling point                   | 10. Condenser                     |
| 11. Saturator                       | 12. Furnace                       |
| 13. Reactor                         | 14. Catalyst bed                  |
| 15. Temperature controller          | 16. Digital temperature indicator |
| 17. Variable voltage transformer    | 18. Thermocouple/Thermometer      |
| 19. Pressure regulator              | 20. Water bath                    |
| 21. Heating and stirring controller |                                   |

**Figure 4.2** Schematic diagram of the reaction apparatus for reaction.

# CHAPTER V

## RESULTS AND DISCUSSION

In this chapter, the results and discussion are divided into the two main parts. First, characterization of the H/MFI, the fresh Ga/MFI catalyst and the pretreated Ga/MFI catalyst for various particle sizes by X-Ray diffraction, SEM, BET, XRF,  $^{27}\text{Al}$  MAS NMR and  $\text{NH}_3$ -TPD are described in section 5.1. Secondly, the catalytic behavior on ethanol aromatization is explained in section 5.2.

### 5.1 Characterization of the catalysts

The commercial catalysts used in this work were first characterized to overview the difference of their characteristics and properties. The structure and crystallinity of MFI catalyst were measured by XRD. The specific surface area and amount of Si, Al and Ga in catalysts were measured to investigate their physical properties. The morphology was determined by SEM. The acidity of catalyst was investigated by  $\text{NH}_3$ -TPD. Finally,  $^{27}\text{Al}$  MAS NMR was tested to observe the structure of aluminum in the sample as solid form.

#### 5.1.1 X-Ray Diffraction pattern

The structure and crystallinity of Ga/MFI catalysts with various particle sizes before and after pretreatment were analyzed by X-ray diffraction (XRD). The XRD patterns of all 1.0, 1.9, 3.2, 4.1 and 6.0  $\mu\text{m}$  Ga/MFI catalysts were the same as expected because all of catalysts used in this study were prepared from the same MFI zeolite structure. Hence, the MFI crystal structure should not be affected by particle size. The commercial catalyst X-ray diffraction line is shown in figure 5.1. The X-ray diffraction lines of 1.0, 1.9, 3.2, 4.1 and 6.0  $\mu\text{m}$  Ga/MFI catalysts with and without hydrothermal treatment are depicted in figures 5.2 and 5.3. No change of MFI structure was observed for various particle size and hydrothermal treatment. However, from the comparison of XRD patterns between the fresh and pretreated catalysts,

there were obvious losses of XRD intensities particularly in large particle size (3.2, 4.1 and 6.0  $\mu\text{m}$ ) of Ga/MFI catalysts.

### 5.1.2 Morphology

Scanning Electron Microscopy (SEM) photographs of the prepared catalysts are shown in Figures 5.4-5.9. The shapes of the all catalysts are roughly crystallized spherical particles which are composed of many small regular plates. The particle sizes of the zeolite samples were measured from Scanning Electron Microscopy by average the diameter of particle. Particle size values estimated from SEM images of the catalyst have been reported in much research investigation (Shichi et al, 2000). Consideration of the SEM photographs depicted in figure 5.5-5.9 indicated the diameters of Ga/MFI zeolite samples were 1.0, 1.9, 3.2, 4.1 and 6.0  $\mu\text{m}$ .

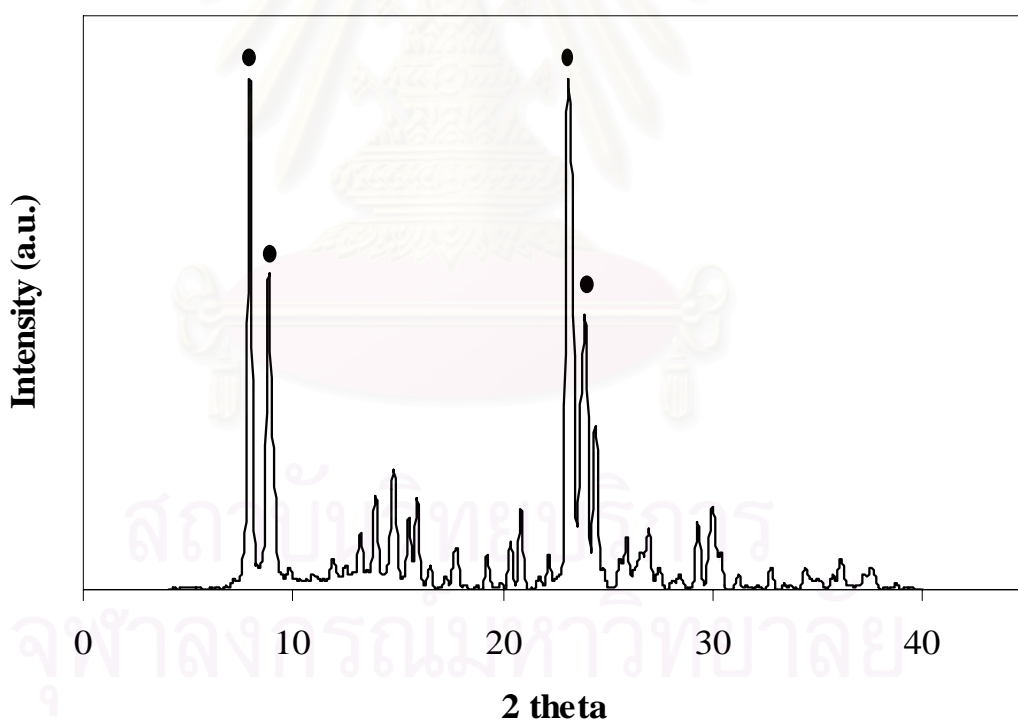


**Figure 5.1** X-ray Diffraction patterns of commercial MFI zeolite.

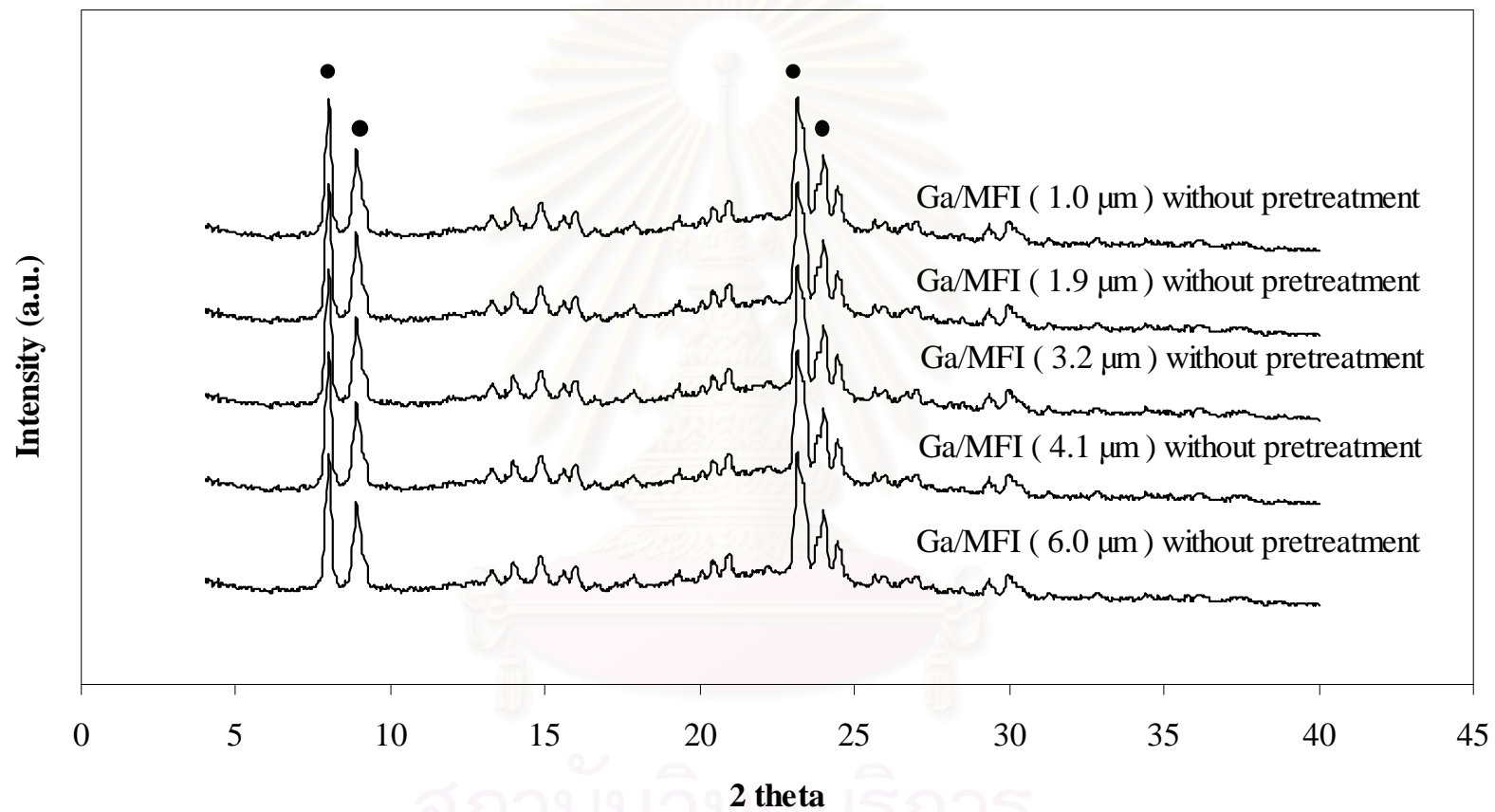
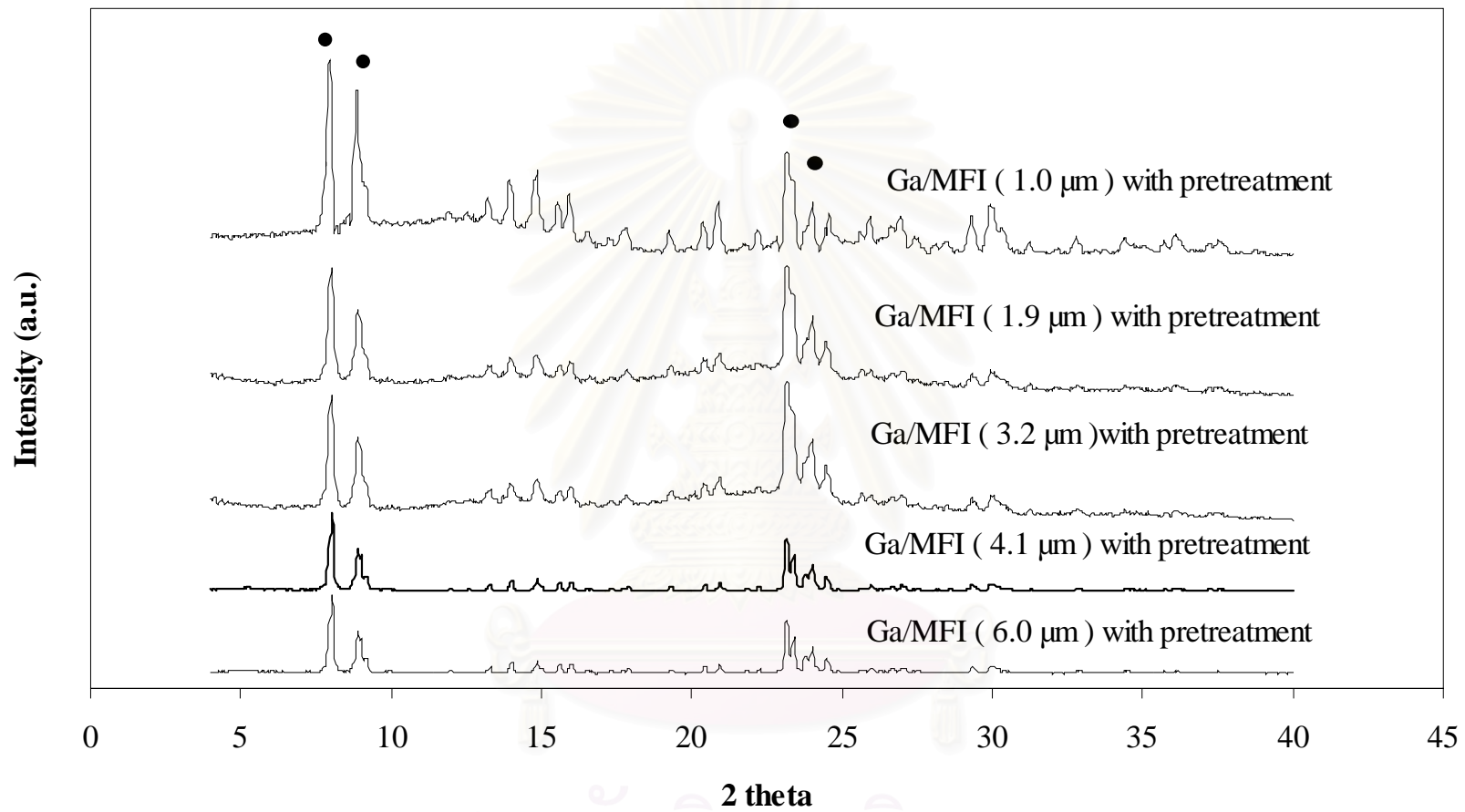
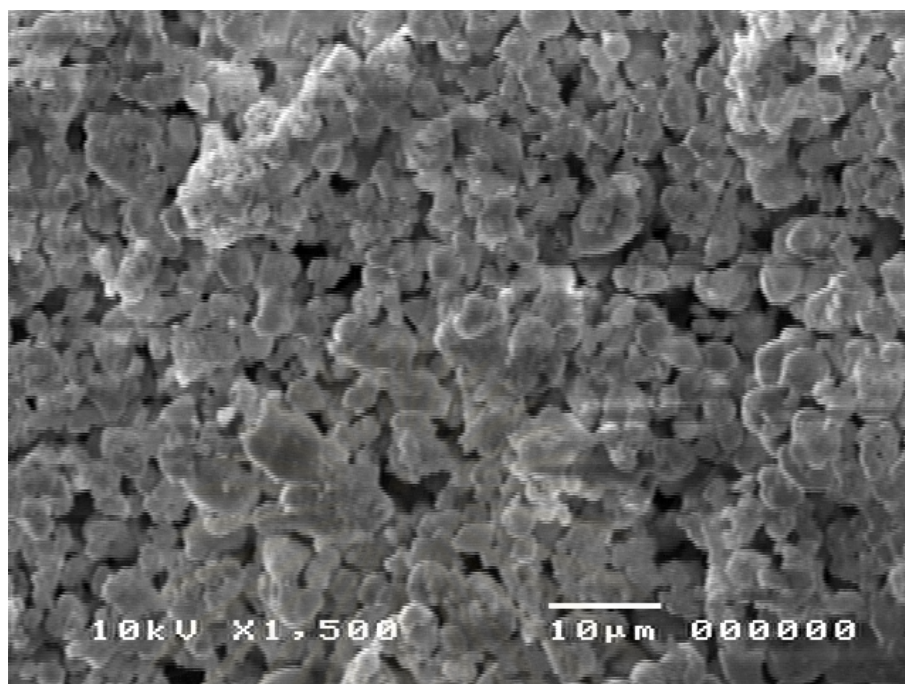


Figure 5.2 X-ray Diffraction patterns of Ga/MFI catalysts.



**Figure 5.3** X-ray Diffraction patterns of Ga/MFI catalysts pretreated at 800 °C with 10% H<sub>2</sub>O for 24 h.



**Figure 5.4** Scanning electron micrograph of Ga/MFI (1.9  $\mu\text{m}$ ) catalyst.

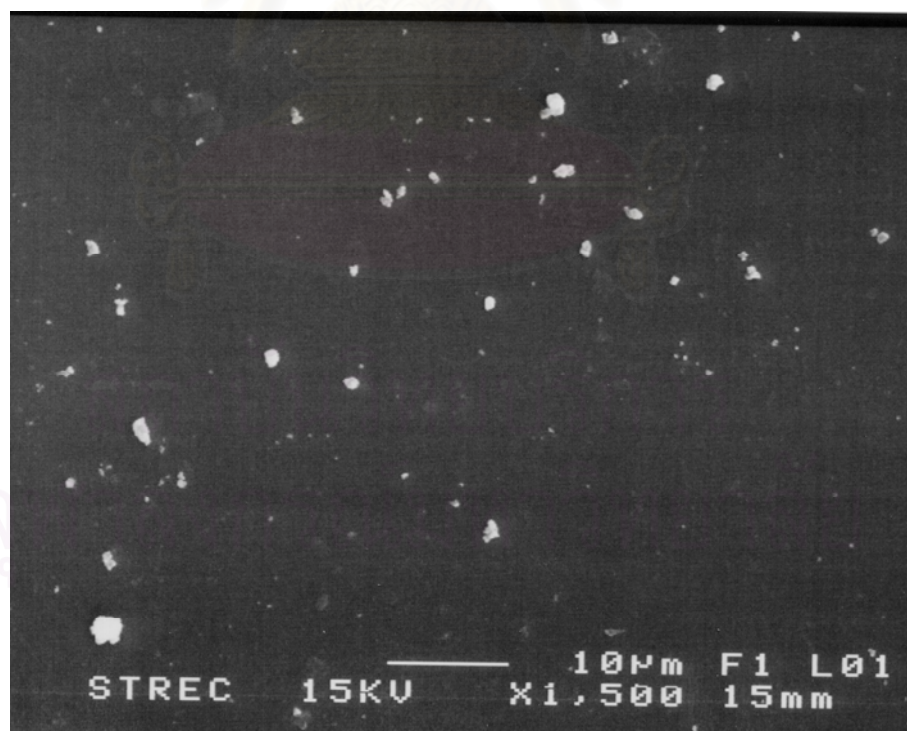


**Figure 5.5** Scanning electron micrograph of Ga/MFI (1.0  $\mu\text{m}$ ) catalyst.

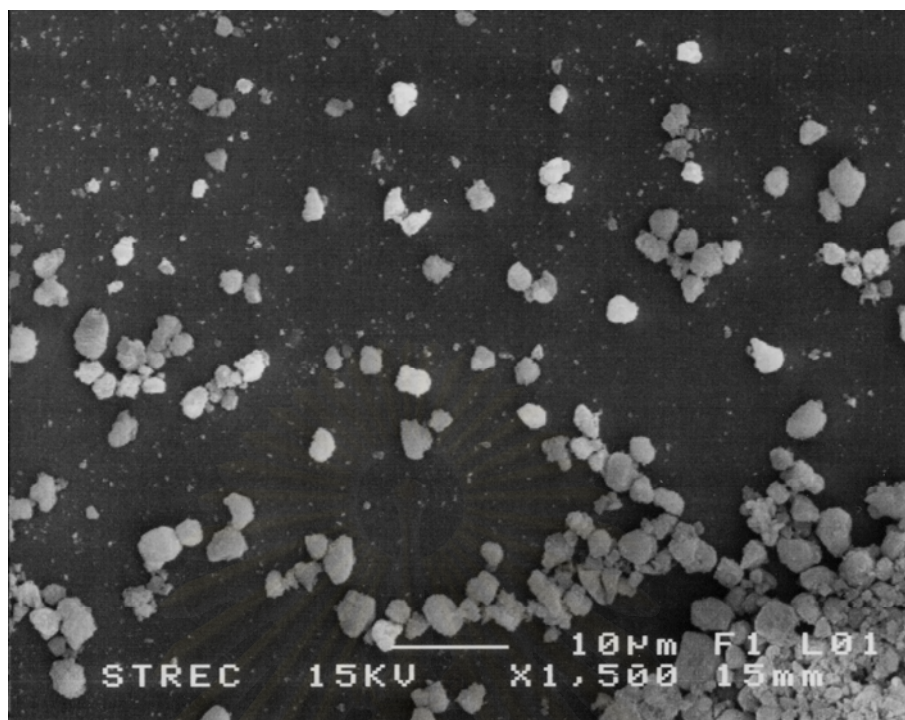


**Figure 5.6** Scanning electron micrograph of Ga/MFI (1.9 μm) catalyst.

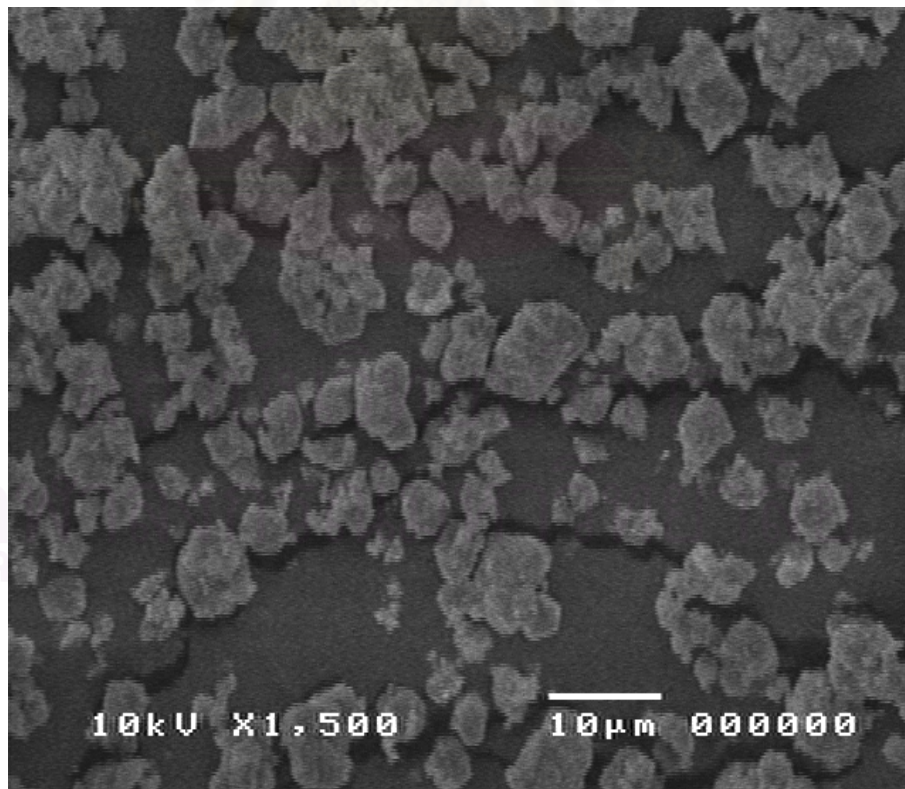


**Figure 5.7** Scanning electron micrograph of Ga/MFI (3.2 μm) catalyst.





**Figure 5.8** Scanning electron micrograph of Ga/MFI (4.1 μm) catalyst.



**Figure 5.9** Scanning electron micrograph of Ga/MFI (6.0 μm) catalyst.

### 5.1.3 Physical Properties

The physical properties of the pretreated and unpretreated catalysts were summarized in Table 5.1. The specific surface area estimated by BET and composition of catalysts in this study were determined. BET surface area is reduced with the presence of pretreatment condition. Table 5.1 showed the zeolite catalysts with Si/Al ratio 40 varying with particle size at the same level of metal content and Ga loading. Crystallinity, as determined by XRD profiles, was calculated based on the area of main peak compared with that of MFI as a reference. No significant loss of crystallinity was observed on these catalysts except large particle size (3.2, 4.1 and 6.0  $\mu\text{m}$ ) of Ga/MFI catalysts.

### 5.1.4 Dealumination

Figure 5.10 shows the  $^{27}\text{Al}$  MAS NMR spectra of fresh Ga/MFI and pretreated Ga/MFI for various particle sizes. The observed spectra confirmed that severe steam treatment causes dealumination. The catalysts exhibited two signals at approx. 60ppm, which is assigned to the tetrahedral aluminum, and at approx. 0ppm, which is attributed to the extra lattice octahedral aluminum in the zeolite lattice (Budi,P., and Howe, R.F.,1997). For the small particle size, sample Ga/MFI (1.0  $\mu\text{m}$ ) and Ga/MFI (1.9  $\mu\text{m}$ ), there are no significant changes in the  $^{27}\text{Al}$  MAS NMR spectra for the fresh and pretreated catalysts. On the other hand, the large particle size catalysts, Ga/MFI (4.1  $\mu\text{m}$ ) and Ga/MFI (6.0  $\mu\text{m}$ ), showed a loss of tetrahedral aluminum but an increase in octahedral aluminum after hydrothermal treatment. This is consistent with a previous report that a loss in activity and durability results after steam pretreatment was due to framework dealumination of the zeolite (Budi, P., 1997). Based on  $^{27}\text{Al}$  MAS NMR signals, the results obtained for the stabilization of the tetrahedral aluminum by different particle size are summarized in table 5.1. After hydrothermal treatment of the catalysts, the relative area of tetrahedral  $^{27}\text{Al}$  is decreased similarly in accord with the BET surface area and crystallinity. It can be concluded that for the small particle size catalysts, Ga/MFI (1.0  $\mu\text{m}$ ) and Ga/MFI (1.9  $\mu\text{m}$ ), the zeolite framework structure is stabilized, preventing the occurrence of dealumination.

**Table 5.1** Physical properties of various particle sizes of Ga/MFI catalysts.

Catalysts	Particle diameter by SEM ( $\mu\text{m}$ )	Si/Al atomic ratio	Ga/Al atomic ratio	BET surface area ( $\text{m}^2/\text{g}$ )		%Cryatallinity		The relative area of tetrahedral $^{27}\text{Al}$ (%)	
				Fresh	Pretreated	Fresh	Pretreated	Fresh	Pretreated
H/MFI-5 ( 1.9 $\mu\text{m}$ )	2.0	39.8	-	354	310	93	80	-	-
Ga/MFI-5 ( 1.0 $\mu\text{m}$ )	1.0	38.6	0.530	309	306	93	91	86	84
Ga/MFI-5 ( 1.9 $\mu\text{m}$ )	1.9	39.2	0.526	367	358	94	91	84	81
Ga/MFI-5 ( 3.2 $\mu\text{m}$ )	3.2	38.8	0.566	328	318	97	89	81	74
Ga/MFI-5 ( 4.1 $\mu\text{m}$ )	4.1	40.7	0.551	333	314	96	84	78	68
Ga/MFI-5 ( 6.0 $\mu\text{m}$ )	6.0	40.1	0.545	315	279	95	83	79	66

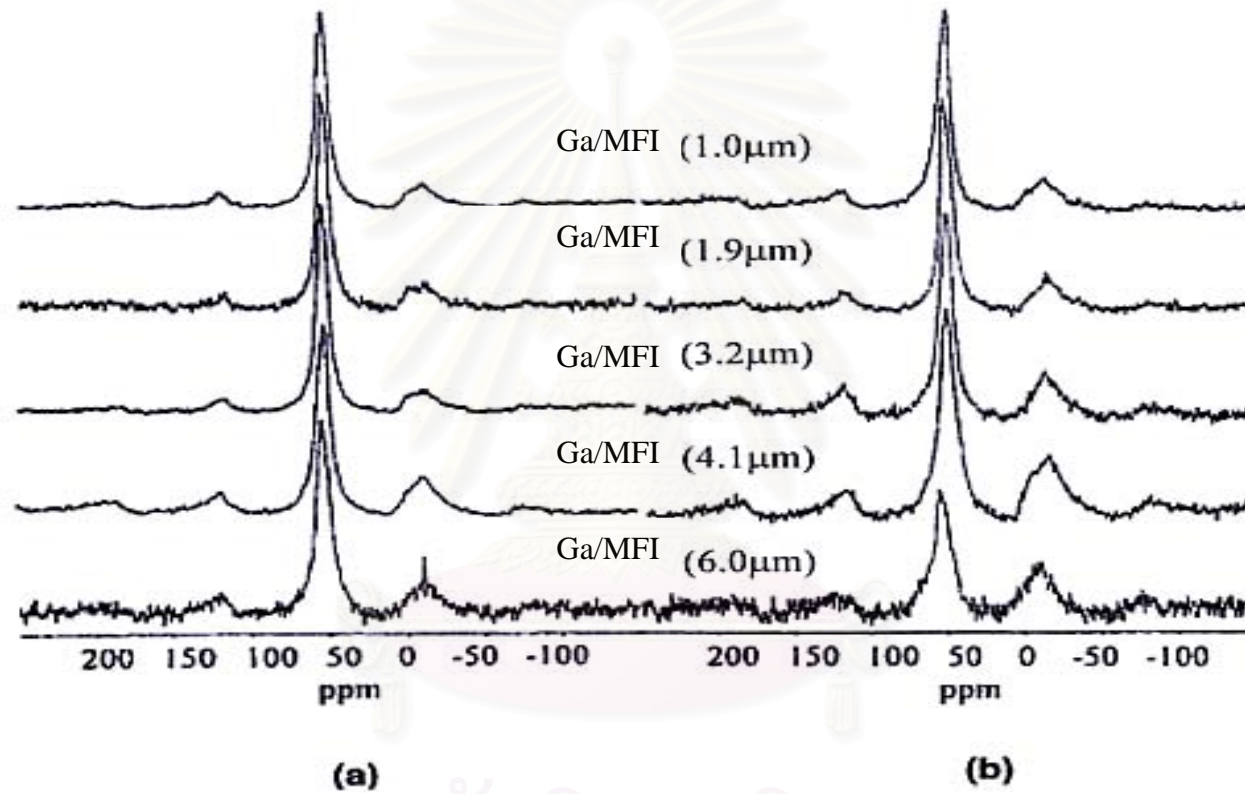
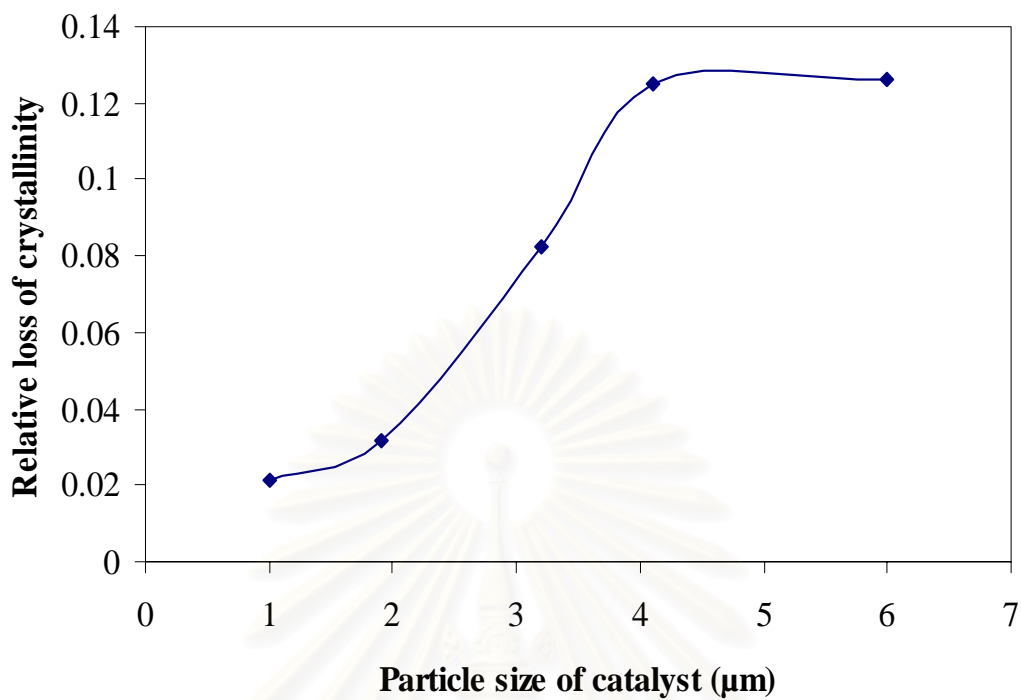


Figure 5.10 <sup>27</sup>Al MAS NMR spectra of Ga/MFI (a) fresh and (b) pretreated catalysts.

The same dependence for the relative loss of crystallinity and the relative loss of tetrahedral aluminum on particle size are shown in figures 5.11 and 5.12 respectively. The relative loss of crystallinity and tetrahedral aluminum are defined as the difference between fresh and pretreated catalysts per fresh catalyst. After hydrothermal treatment, the small particle size catalyst showed a slight decrease in crystallinity and moderate loss of tetrahedral aluminum while the large particle size catalysts lost a considerable amount of their crystallinity and their tetrahedral aluminum, which resulted in lower durability in the case of large particle size catalysts. However, the reason for less dealumination for the smaller particle size catalysts is still unclear. It might be expected that the large particle size catalyst may have many defect points compared with the small size catalyst. Consequently, further studies which aim at clearly describing the influence of particle size effects on durability are warranted.





**Figure 5.11** The effect of particle size on the relative loss of crystallinity.

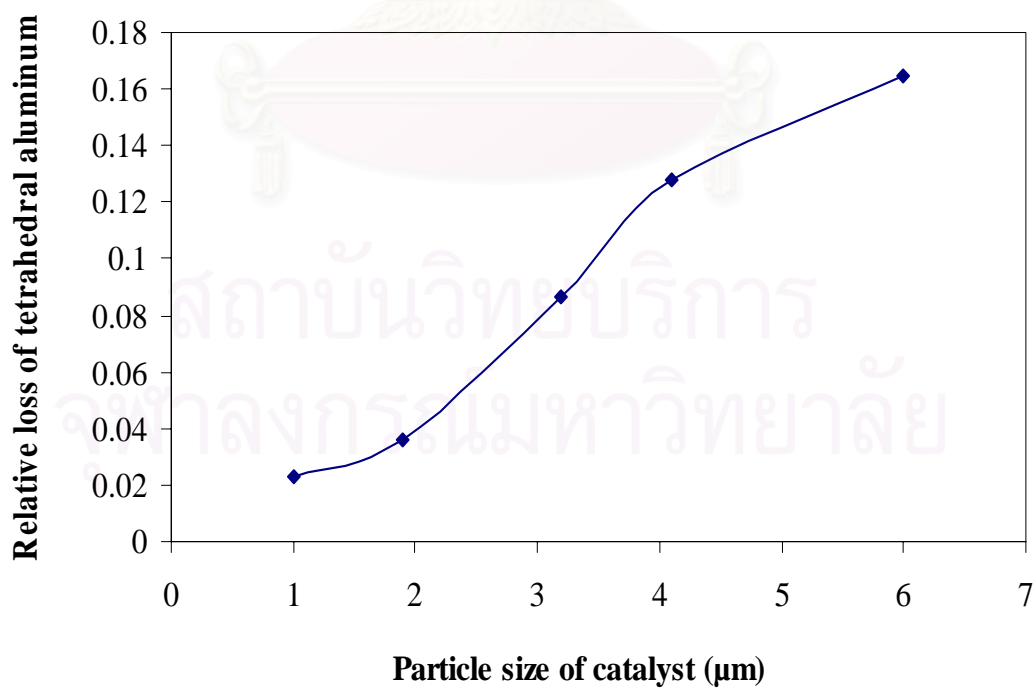


**Figure 5.12** The effect of particle size on the relative loss of tetrahedral aluminum.

### 5.1.5 Temperature Programmed Desorption of Ammonia (NH<sub>3</sub>-TPD)

The TPD profiles of desorbed NH<sub>3</sub> from fresh and pretreated catalysts are shown in Table 5.2. The profiles are composed of two peaks, i.e., a high temperature peak of strong acid sites and a low temperature peak of weak acid sites (Inui, T., 1984).

**Table 5.2** The peak concentration of acid sites of the various particle size.

condition	Catalyst	Weak Acidity (mmole/g.cat )	Temperature of weak acidity	Strong Acidity (mmole/g.cat )	Temperature of strong acidity
Fresh	H/MFI-5 (1.9 μm)	0.59	175	0.36	386
	Ga/MFI-5 (1.0 μm)	0.54	168	0.22	383
	Ga/MFI-5 (1.9 μm)	0.52	173	0.29	409
	Ga/MFI-5 (3.2 μm)	0.51	169	0.31	395
	Ga/MFI-5 (4.1 μm)	0.57	168	0.26	390
	Ga/MFI-5 (6.0 μm)	0.54	166	0.20	385
Pretreated	H/MFI-5 (1.9 μm)	0.39	160	-	-
	Ga/MFI-5 (1.0 μm)	0.51	156	-	-
	Ga/MFI-5 (1.9 μm)	0.48	172	-	-
	Ga/MFI-5 (3.2 μm)	0.46	169	-	-
	Ga/MFI-5 (4.1 μm)	0.45	163	-	-
	Ga/MFI-5 (6.0 μm)	0.38	160	-	-

From figure 5.13 show the NH<sub>3</sub>- TPD profile of fresh Ga/MFI catalysts for various particle sizes which consisted of a high temperature peak of strong acid sites and a low temperature peak of weak acid sites. After Ga/MFI catalysts are pretreated with 10% H<sub>2</sub>O for 24 h, the NH<sub>3</sub>- TPD profiles are indicated loss strong acid site as shown in figure 5.14.

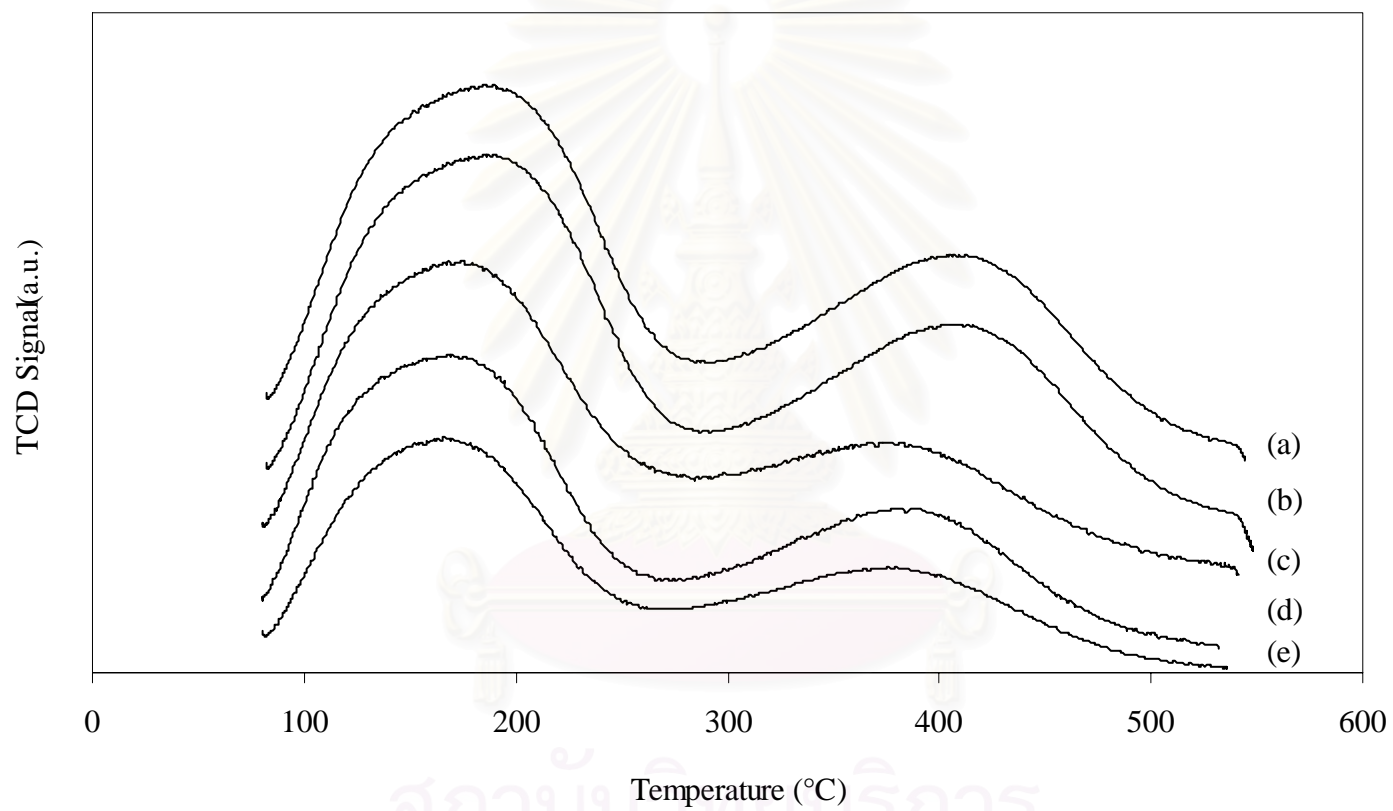


**Figure 5.13** The Temperature Programmed Desorption Profile of fresh Ga/MFI catalysts for various particle sizes (a) 1.0 μm (b) 1.9 μm (c) 3.2 μm (d) 4.1 μm (e) 6.0 μm.



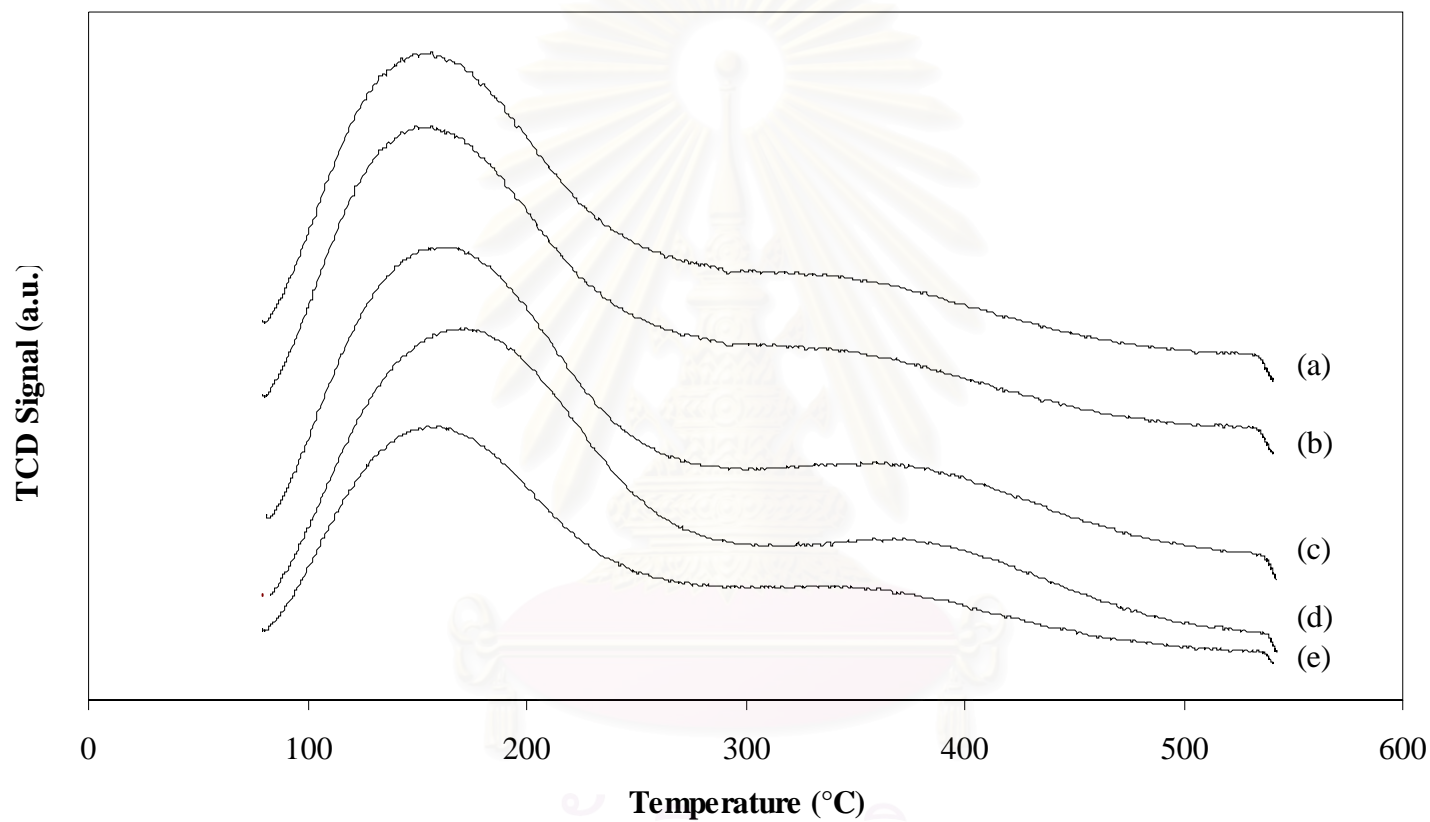


**Figure 5.14** The Temperature Programmed Desorption Profile of pretreated Ga/MFI catalysts for various particle sizes (a) 1.0  $\mu\text{m}$  (b) 1.9  $\mu\text{m}$  (c) 3.2  $\mu\text{m}$  (d) 4.1  $\mu\text{m}$  (e) 6.0  $\mu\text{m}$ .

A similar dependence for the relative loss of crystallinity and the relative loss of acidity on particle size are shown in figure 5.15. The relative loss acidity was defined as the difference between fresh and pretreated catalysts per fresh catalyst. After hydrothermal treatment, the large particle size catalysts were decreased slighter than the small particle size catalysts because the large particle size catalysts were loosed a considerable amount of their crystallinity and their tetrahedral aluminum, which resulted in lower tetrahedral aluminum in the case of large particle size catalysts. However, the reason for less dealumination for the larger particle size catalysts is still unclear. It might be expected that the large particle size catalyst may have many defect points compared with the small size catalyst. Consequently, further studies which aim at clearly describing the influence of particle size effects on acidity are warranted.

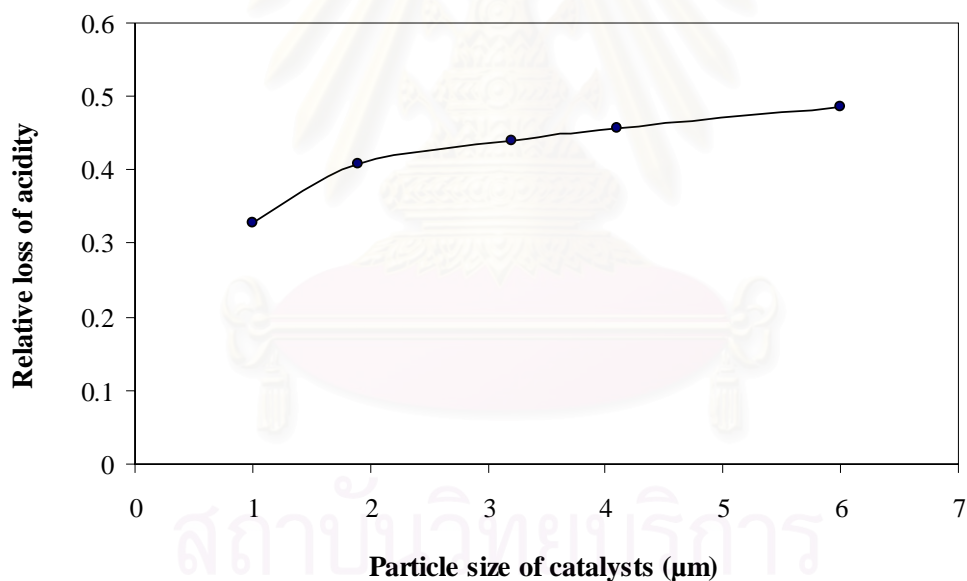


**Figure 5.15** The effect of particle size on the relative loss of acidity.

## 5.2 Catalytic Reaction

In this section, the catalytic properties of the catalysts prepared in this research are investigated by testing the aromatization of ethanol (20wt% ethanol).

### 5.2.1 The effect of acidity and Gallium on the selectivity of aromatics

The effect of acidity and gallium to ethanol aromatization were compared. The aromatic selectivity increased after loading gallium on MFI catalysts because the Ga-species in the presence of zeolitic protons were facilitate dehydrogenation reactions which control the formation of aromatic hydrocarbons (Vasant, R.C., et al. 2001). Although the acidity of the Ga/MFI pretreated catalysts decreased, the aromatic selectivity on ethanol aromatization still increased. The results obviously demonstrated that gallium in MFI catalyst affected aromatic selectivity higher than acidity on ethanol conversion to aromatics as shown in figure 5.16.

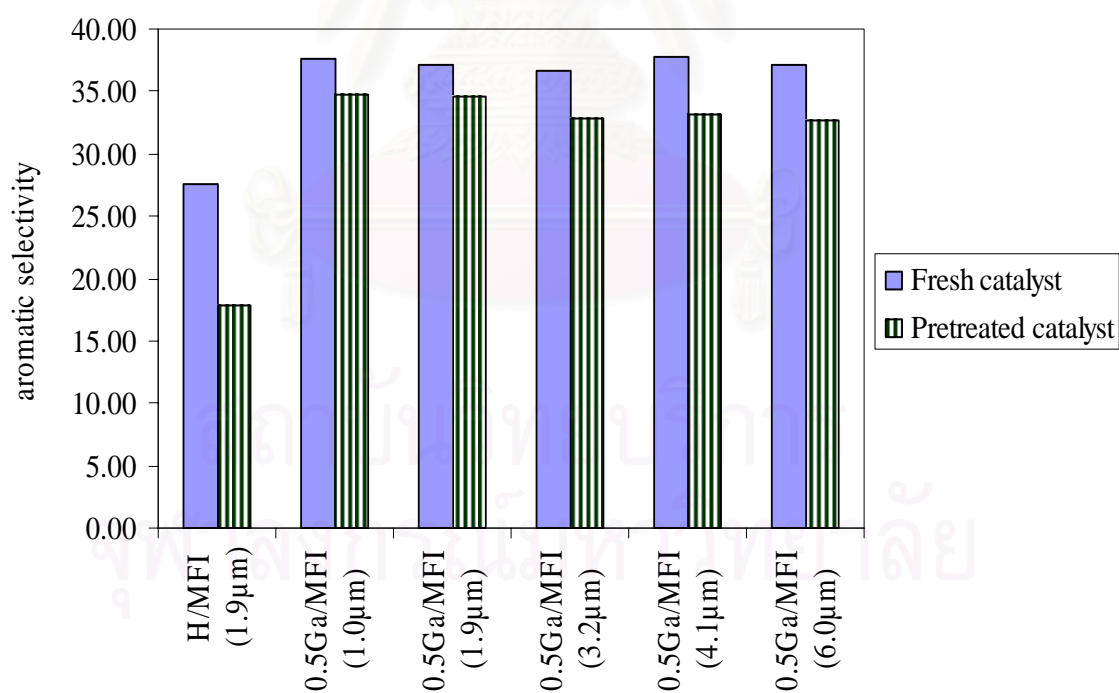


**Figure 5.16** The effect of acidity and Gallium on the selectivity of aromatics.

### 5.2.2 The effect of acidity on the selectivity of aromatics(BTX)

The fresh Ga/MFI catalysts had strong acid sites and weak acid sites while the pretreated Ga/MFI catalysts had only weak acid site. As mentioned above, it is evident that the small particle size of Ga/MFI catalysts showed a moderate decrease in acidity while the large particle size of Ga/MFI catalysts lost extensive acidity. The influence of acidity on ethanol conversion to aromatics was examined high selectivity of benzene, toluene and xylene as shown in figure 5.17 and figure 5.18. The small particle size of catalysts increased benzene and toluene selectivity but decreased xylene selectivity because the small particle size still had acidity. On the other hand, the large particle size had less acidity which results in lower benzene and toluene selectivity and higher xylene selectivity.

### 5.2.3 The effect of acidity on the selectivity of olefins

Although the acidity of the pretreated Ga/MFI catalysts decreased, the olefin selectivity stills the same because the acidity of all Ga/MFI (fresh and pretreated) catalysts were enough to convert ethanol to olefins as shown in figure5.17 and figure 5.18 .

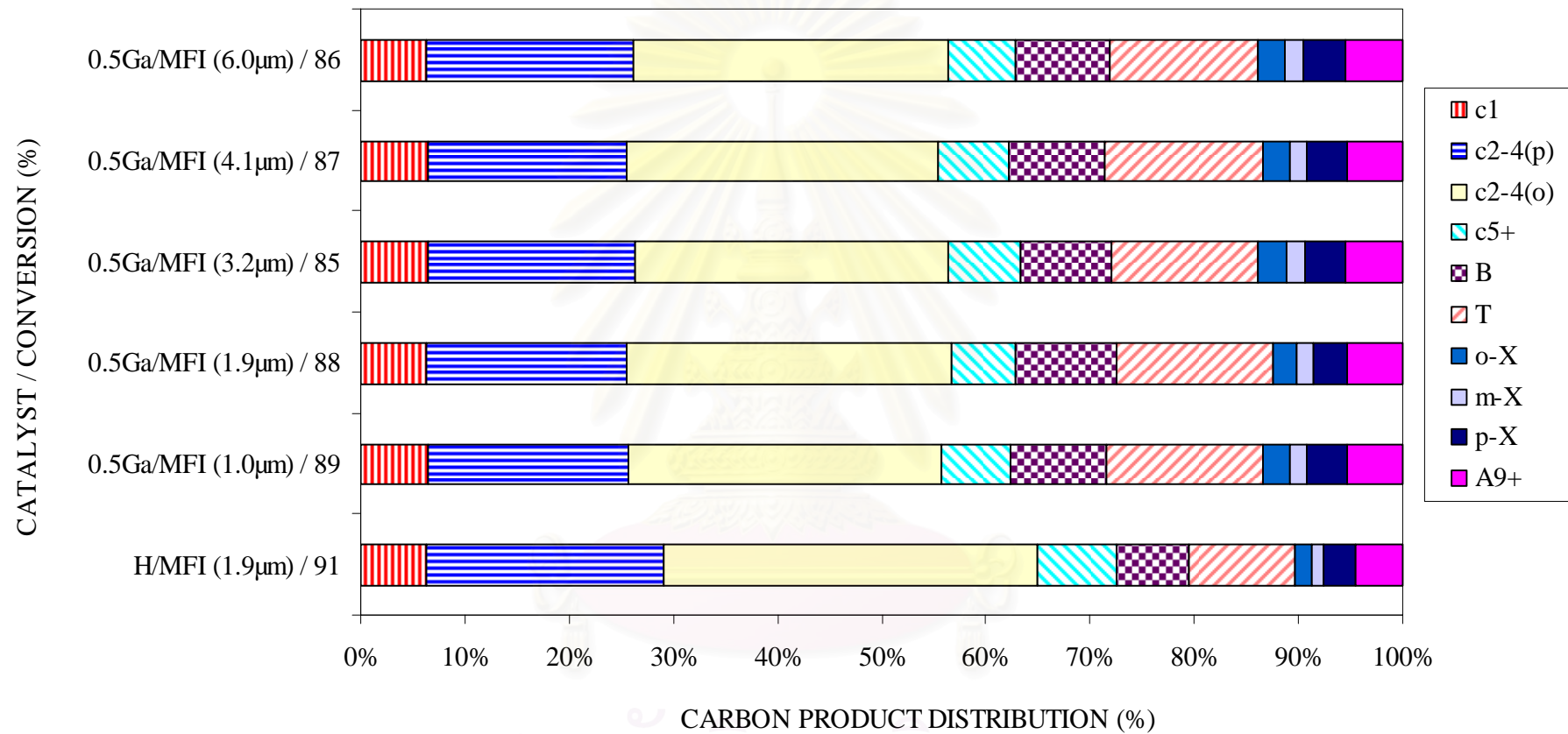


**Figure 5.17** The selectivity of fresh catalyst on ethanol aromatization.

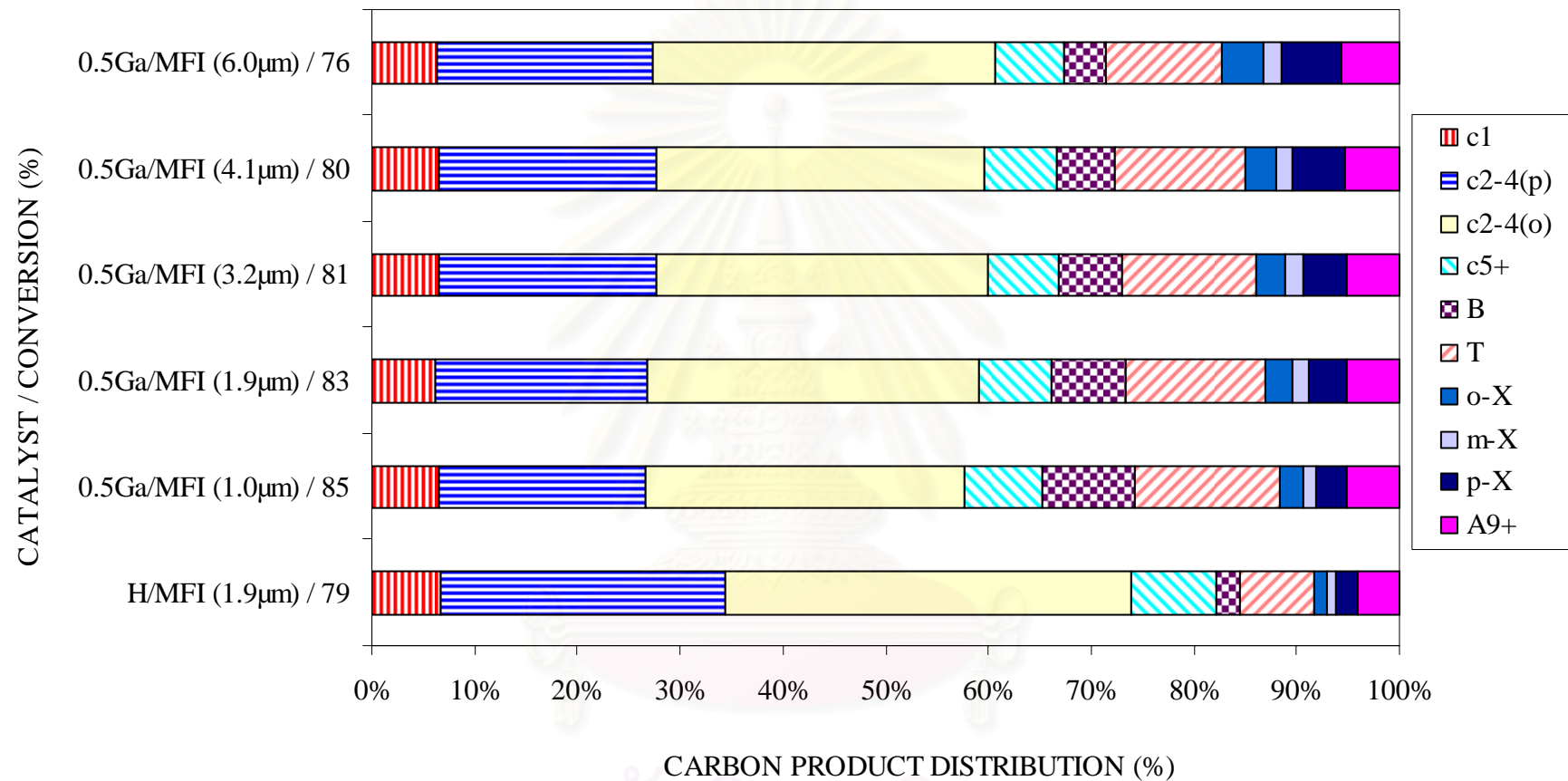


**Figure 5.18** The selectivity of pretreated catalyst on ethanol aromatization

## CHAPTER VI

### CONCLUSIONS AND RECOMMENDATIONS

#### 6.1 CONCLUSIONS

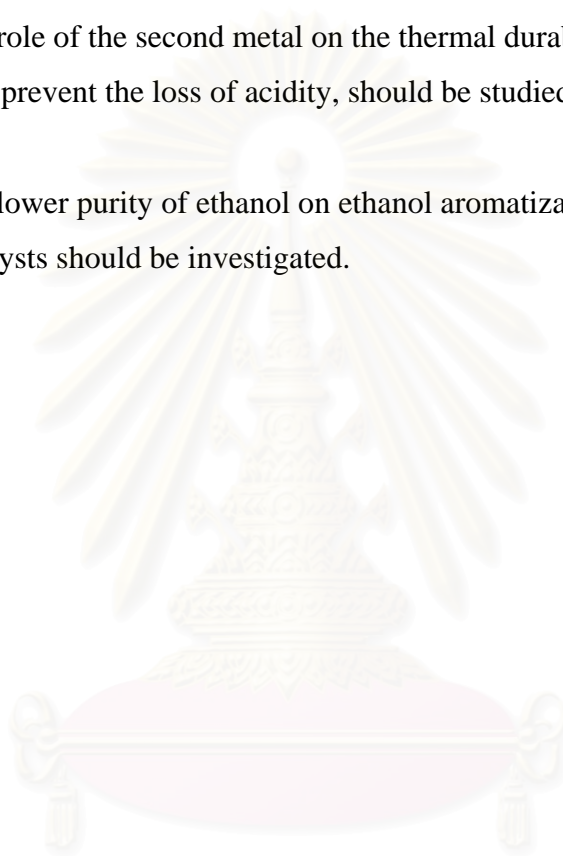
In this thesis, the various particle sizes of Ga/MFI zeolite catalyst were synthesized and tested on ethanol conversion to aromatics. The conclusions of this research were summarized as follow:

1. The smaller particle size Ga/MFI zeolite exhibited the greater durability for hydrothermal treatment condition. The smaller particle size catalysts showed a slight decrease in crystallinity whereas the large crystal size catalysts lost considerable crystallinity.
2. The gallium in MFI catalyst affected aromatic selectivity higher than acidity on ethanol conversion to aromatics.
3. The small particle size of catalysts increased benzene and toluene selectivities but decreased xylene selectivities because the small particle size still had acidity. On the other hand, the large particle size had less acidity which results in lower benzene and toluene selectivities and higher xylene selectivity.
4. Although the acidity of the pretreated Ga/MFI catalysts decreased, the olefin selectivity stills the same because the acidity of all Ga/MFI (fresh and pretreated) catalysts was enough to convert ethanol to olefins.

## 6.2 RECOMMENDATION

From this research, the recommendations for further study are as follows:

1. Further studies which aim at the effect nano particle size of MFI catalyst on ethanol conversion to aromatics should be investigated.
2. The role of the second metal on the thermal durability of zeolite, in which they prevent the loss of acidity, should be studied.
3. The lower purity of ethanol on ethanol aromatization with modify MFI catalysts should be investigated.



สถาบันวิทยบริการ  
จุฬาลงกรณ์มหาวิทยาลัย

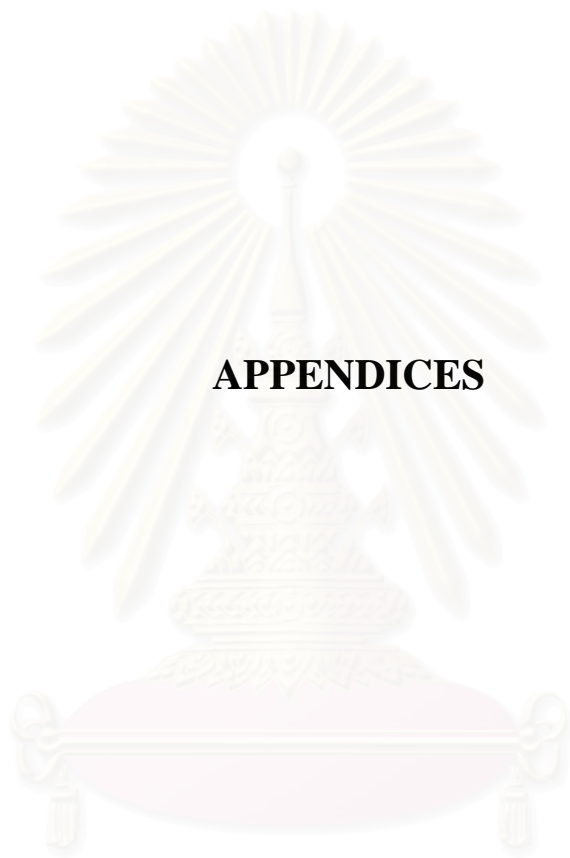


## REFERENCES

- Ashton, A.G.; Batamian, S.; and Dwyer, J. Acid in Zeolite (Imelik, B. et al.). Catalysis by Acid-Bases, Amsterdam: Elsevir, 1985.
- Barthoment, D. Acidic catalysts with Zeolites. Zeolites Science and Technology (Rebeira, F.H. et al.), Martinus Nijhoff Publishers, The Hange, 1984.
- Barrer, R.M. Hydrothermal Chemistry of zeolites, London: AcedamicPress, 1982.
- Bekkm, H.V.; Flanigen, E.M.; and Jansen, J.C. STM image of silicalite-1 pore structure. Stud.Surf.Sci. Catal. 578 (1991).
- Bhaskar, G.V.; and Do, D.D. Toluene disproportionation reaction over HZSM-5 zeolites. Kinetics and mechanism. Industrial and Engineering Chemistry Research. 29 (3) (1990): 355-361.
- Budi, P.; and Howe, R.F. Steam deactivation of CoZSM-5 NO<sub>x</sub> reduction catalysts. Catal. Today. 38 (1997): 175.
- Chang, C.D. Hydrocarbons from methanol. Catal.Rev.-Sci.Eng. 25 (1983(1)): 9.
- Chau-Shang, C.; and Min-Dar, L. Effect of hydrogen pretreatment on catalytic properties of Ga/ZSM-5 catalyst. React.Kinet.Catal.Lett. (1) (1995): 115-120.
- Chen, D.; Moljord, K.; Fuglerud, T.; and Holmen, A. The effect of crystal size of SAPO-34 on the selectivity and deactivation of the MTO reaction. Micropor. Mesopor. Meter. 29 (1999): 191.
- Choudhary, V.R.; Kinage, A.K.; and Choudhary, T.V. Direct aromatization of natural gas over H-gallosilicate (MFI), H-galloaluminosilicate (MFI) and Ga/H-ZSM-5 zeolites. Appl.Catal.A. 162 (1997): 239-248.
- Hatch, L. F.; and Mater, S. From hydrocarbons to petrochemicals – 14.chemicals from methylbenzenes. Hydrocardon Process. 58(1) (1979): 189.
- Inui, T.; Yamase, O.; Fugada, K.; Itoh, A.; Tarmuto, J.; and Morina, T.Y. Proceeding 8<sup>th</sup> Internation Congress on Catalysis, Berlin, Vol.3, Dechema Frankfult-am-Main, 1984.
- King, R.B. Encyclopedia of Inorganic Chemistry, (1994): 4365-4391.
- Kumer, N.; And Lindfors, L.E. Modification of the ZSM-5 zeolite using Ga and Zn impregnated silica fibre for the conversion of n-butane into aromatic hydrocarbons. Catal Lett. 38 (1996): 239-244.

- Lee, M.D.; and Chang, C.S. Effects of hydrogen pretreatment on the acidic and catalytic properties of gallium-supported H-ZSM-5 in n-hexane aromatization. Appl. Catal. A. 123 (1995): 7-21.
- Meier, W.M.; and Olson, D.H. Atlas of Zeolite Structure Types, 3<sup>rd</sup> revised ed., int. Zeolite Assoc., Boston: Butterworth-Heiemann, 1992.
- Pines, H. The Chemical of catalytic Hydrocarbon Conversion. New York: Academic, 1981.
- Sadeghbeigi, R. Fluid Catalytic Cracking Handbook. Gulf Publishing Company, 2000.
- Sano. T.; Fujisawa, K.; and Higiwara, H. High Stream Stability of H-ZSM-5 Type Zeolite Containing Alkaline Earth Metals Catalyst Deactivation, (Delmon, B. and Froment, G.R. eds), Stud. Surf. Sci. Catal., Amsterdam: Elsevier. (1987): 34.
- Satterfield, C.N. Heterogeneous Catalysis in Industrial Practice, 2<sup>nd</sup> ed., New York: McGraw-Hill. (1991): 226-259.
- Shichi, A.; Katagi, K.; Satsuma, A.; and Hattori, T. Influence of intracrystalline diffusion on the selective catalytic reduction of NO by hydrocarbon over Cu-MFI zeolite. Appl. Catal. B. 24 (2000): 97.
- Shichi, A.; Satsuma, A.; Iwase, M.; Shimizu, K.; Komai, S.; and Hattori, T. Catalyst effectiveness factor of cobalt-exchanged mordenites for the selective catalytic reduction of NO with hydrocarbons. Appl. Catal. B. 179 (1998): 107.
- Szoztak, R. Molecular Sieve Principle of Synthesis and Identification, New York: Van Nostrand Reingold. (1989): 1-50.
- Tanake, K.; Misona, M.; Ona, Y.; and Hattori, H. New Solid Acids and Bases. Stud. Surf. Sci. Catal. Tokyo: Elsevier. (1989): 51.
- Vasant, R.C.; Kshudiram, M.; and Sivadinarayana, C. Influence of zeolite factors affecting zeolitic acid on the propane aromatization activity and selectivity of Ga/H-ZSM-5. Microporous and Mesoporous Mater. 37 (2000): 21-27.
- Vasant, R.C.; Panjala, D.; Subhabrata, B.; and Anil, K.K. Aromatization of dilute ethylene over Ga-modified ZSM-5 type zeolite catalysts. Microporous and Mesoporous Mater. 47 (2001): 253-267.

- Viswanadham, N.; Pradhan, A.R.; Ray, N.; Visknoi, S.C.; Shanker, U.; and Prasada Rado, T. S. R. Reaction pathways for the aromatization of paraffins in the presence of H-ZSM-5 and Zn/H-ZSM-5. Appl. Catal. A. 137 (1996): 225-233.
- Wittcoff, H.A. The Chemical Industry: Technology and concepts, Chem. System Inc., Union Chem. Lab, Ind.Tech. Res. Inst., Hsin Chu, Taiwan. 12-13 March, 1992.
- Xeudong, L.; and Shaoyi, P. Modification of HZSM-5 by metal surfactant for aromatization. Microporous and Mesoporous Mater. 25 (1998): 201-206.
- Zaihui, F.; Dulin, Y.; Yashu, Y.; and Xiexian, G. Characterization of modified ZSM-5 catalysts for propane aromatization prepared by a solid state reaction. Appl. Catal. A. 124 (1995): 59-71.
- Zeshan, H.; Yonggang, S.; Chuanghui, L.; Songyang, C.; Jingxiu, D.; Iordache, O.M.; Maria, G.C.; and Pop, G.L. The source of HCl emission from municipal refuse incinerators. Ind.Eng-Chem.Res. 27 (1988): 2218.



**APPENDICES**

สถาบันวิทยบริการ  
จุฬาลงกรณ์มหาวิทยาลัย

## APPENDIX A

### SAMPLE OF CALCULATIONS

#### A-1 Calculation of Si/Al Atomic Ratio for MFI

The calculation is based on weight of sodium Silicate ( $\text{Na}_2\text{O SiO}_2 \text{H}_2\text{O}$ ) in B1 and B2 solution.

M.W. of Si	=	28.0855
M.W. of $\text{SiO}_2$	=	60.0843
Weight percent of $\text{SiO}_2$ in sodium Silicate	=	28.5
M.W. of Al	=	26.9815
M.W. of $\text{AlCl}_3$	=	133.3405
Weight percent purity of $\text{AlCl}_3$	=	97

For example, to prepare MFI at Si/Al atomic ratio of 40.

Using Sodium Silicate 69 g with 45 g of water as B1 solution.

$$\begin{aligned}\text{Mole of Si used} &= \frac{\text{wt.(\%)} \times (\text{M.W. of Si}) \times (1\text{mole})}{100 \quad (\text{M.W. of SiO}_2) \quad (\text{M.W. of Si})} \\ &= 69 \times (28.5/100) \times (1/60.0843) \\ &= 0.3273\end{aligned}$$

Si/Al atomic ratio = 40

$$\begin{aligned}\text{Mole of AlCl}_3 \text{ required} &= 0.3273/40 \\ &= 8.1825 \times 10^{-2} \text{ mole} \\ \text{amount of AlCl}_3 &= 8.1825 \times 10^{-2} \times 133.34 (100/97) \\ &= 1.125 \text{ g}\end{aligned}$$

which used in A1 and A2 solutions.

### A-2 Calculation of the amount of Ga ion-exchanged MFI

Determine the amount of Ga into catalyst = 0.5 wt.

The catalyst use = x g

$$\text{So that } \frac{\text{Ga}}{(x+\text{Ga})} = 0.5/100$$

$$100 \times \text{Ga} = 0.5 \times (x+\text{Ga})$$

$$(100-0.5) \times \text{Ga} = 0.5x$$

$$\text{thus } \text{Ga} = 0.5x/(100-0.5) \text{ g}$$

use  $\text{Ga}(\text{NO}_3)_3 \cdot 8\text{H}_2\text{O}$  (M.W. 399.83, purity 99.8%)

$$\text{weight of } \text{Ga}(\text{NO}_3)_3 \cdot 8\text{H}_2\text{O} = 0.5x/(100-0.5) \times [(399.83/31) \times (99.8/100)]$$

### A-3 Calculation of particle size from SEM photograph

Diameter sizes measured from SEM photograph of the as-synthesized product of the H/MFI catalysts were calculated as follow,

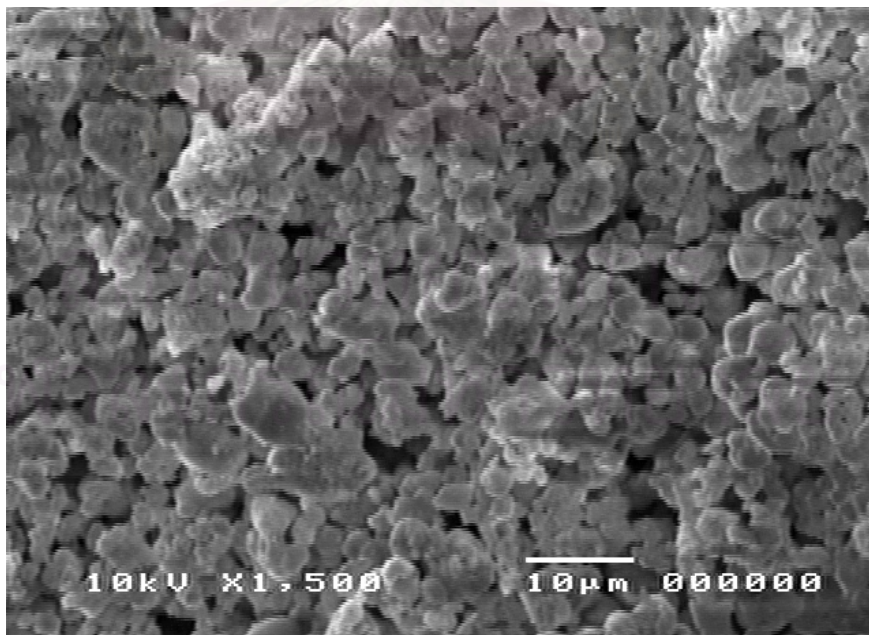


**Figure A1** Scanning electron micrograph of H/MFI (2.0 μm) catalyst.

At x 1,500 magnification, the scale is

$$1.6 \text{ cm} = 10 \mu\text{m}$$

From SEM photograph, it was found that the diameter size of particle was 0.5 cm. Therefore, the diameter size observed by SEM is

$$\text{Diameter size} = \frac{10 \mu\text{m} \times 0.5 \text{ cm}}{1.6 \text{ cm}}$$

$$\text{Diameter size} = 3.2 \mu\text{m}$$

The measure diameter sizes from SEM photograph were cm. The average particle size was

$$\begin{aligned} \text{Particle size} &= \frac{3.2 + 1.8 + 1.9 + 2.5 + 3.1 + 1.8 + 1.7 + 2.2 + 2.0 + 1.8}{10} \\ &= 2.0 \mu\text{m} \end{aligned}$$

#### A-4 Calculation of vapor pressure of water

Set the partial vapor pressure of water to the requirement by adjusting the temperature of saturator according to the antoine equation

$$\log P = A - \frac{B}{(T + C)}$$

When P = vapor pressure of water, mbar

T = temperature, °C

A, B and C is constants

Range of temperature that applied ability -20 -126 °C

The values of constants.

Reactant	A	B	C
Water	8.19625	1730.630	233.426

**A-5 Calculation of percent crystallinity**

$$\% \text{ Crystallinity} = \frac{\text{Area under XRD pattern of sample} \times 100}{\text{Area under XRD pattern of reference}}$$

Reference is the fresh commercial MFI

**A-6 Calculation of the relative area of tetrahedral aluminum (%)**

$$\text{The relative area of tetrahedral aluminum (\%)} = \frac{\text{Area of tetrahedral Al} \times 100}{\text{Total Area}}$$

Area of tetrahedral aluminum is a peak at chemical shift of around 60 ppm.

Total area is a summation area of tetrahedral and octahedral aluminum (0 ppm).



สถาบันวิทยบริการ  
จุฬาลงกรณ์มหาวิทยาลัย



## APPENDIX B

### CALCULATIONS OF REACTION FLOW RATE

#### Sample of calculation

The used catalyst = 0.1000 g

Pack catalyst into quartz reactor (inside diameter = 0.6 cm).

Determine the average high of catalyst bed = H cm, so that,

$$\text{Volume of bed} = \pi (0.3)^2 \times H \text{ ml-cat.}$$

Use Gas Hourly Space Velocity (GHSV) = 2000 h<sup>-1</sup>

$$\text{GHSV} = \frac{\text{Volumetric flow rate}^1}{\text{Volume of bed}}$$

$$\begin{aligned} \text{Volumetric flow rate}^1 &= 2000 \times \text{Volume of bed} \text{ ml/h} \\ &= \frac{2000 \times \pi (0.3)^2 \times H}{60} \text{ ml/min} \end{aligned}$$

At STP condition:

$$\text{Volumetric flow rate} = \text{Volumetric flow rate}^1 \times \frac{(273.15+T)}{273.15}$$

Where T = room temperature

## APPENDIX C

### DATA OF EXPERIMENT

#### Calculation of conversion and hydrocarbon distribution of ethanol conversion reaction

Ethanol conversion activity was evaluated in term of conversion of ethanol into other hydrocarbons

For example: Synthesized H/MFI zeolite  
Reaction condition: reaction temperature 600 °C  
GHSV = 2000 h<sup>-1</sup>  
Feed 20 % ethanol N<sub>2</sub> balance,  
Time on steam = 30 mintute

$$\text{Ethanol conversion (\%)} = \frac{(\text{ethanol}_{\text{in}} - \text{ethanol}_{\text{out}}) \times 100}{\text{ethanol}_{\text{in}}}$$

From data of Shimadza GC 8A (Porapack-Q column)

$$\begin{aligned} \text{Ethanol conversion (\%)} &= \frac{(907450 - 138768) \times 100}{907450} \\ &= 84.71 \% \end{aligned}$$

From data of Shimadza GC 14B ( VZ-10 column)

Area of C <sub>1</sub>	=	45259
Area of C <sub>2</sub>	=	8455
Area of C <sub>2</sub> <sup>=</sup>	=	30196
Area of C <sub>3</sub>	=	27993
Area of C <sub>3</sub> <sup>=</sup>	=	176205
Area of C <sub>4</sub>	=	51298

$$\begin{aligned}
 \text{Area of } i\text{-C}_4 &= 73324 \\
 \text{Area of } \text{C}_4^- &= 18260 \\
 \text{Area of } i\text{-C}_4^- &= 31262 \\
 \text{Area of } \text{C}_5^+ &= 53501 \\
 \text{Area of } \text{C}_1\text{- } \text{C}_5^+ &= \text{summation of area } \text{C}_1 \text{ to area } \text{C}_5^+ \\
 \text{Area of } \text{C}_1\text{- } \text{C}_5^+ &= 660392
 \end{aligned}$$

From data of Shimadza GC 14B (Bentone 34 column)

The first part of data area is  $\text{C}_1\text{- } \text{C}_5^+$ .

$$\begin{aligned}
 \text{Area of } \text{C}_1\text{- } \text{C}_5^+ &= 69710 \\
 \text{Total area} &= 90336
 \end{aligned}$$

So that: compared area form Shimadza GC 14B ( VZ-10 column) and Shimadza GC 14B (Bentone 34 column)

$$\begin{aligned}
 \text{Area of } \text{C}_1(\text{Bentone 34}) &= \frac{\text{Area of } \text{C}_1(\text{VZ-10}) \times \text{Area of } \text{C}_1\text{- } \text{C}_5^+(\text{ Bentone 34})}{\text{Area of } \text{C}_1\text{- } \text{C}_5^+(\text{VZ-10})} \\
 &= \frac{45264 \times 69710}{660392} \\
 &= 4778
 \end{aligned}$$

The other were calculated as the same way

$$\begin{aligned}
 \text{Area of } \text{C}_1(\text{ Bentone 34}) &= 4778 \\
 \text{Area of } \text{C}_2(\text{ Bentone 34}) &= 893 \\
 \text{Area of } \text{C}_2^-(\text{ Bentone 34}) &= 3189 \\
 \text{Area of } \text{C}_3(\text{ Bentone 34}) &= 2955 \\
 \text{Area of } \text{C}_3^-(\text{ Bentone 34}) &= 18600 \\
 \text{Area of } \text{C}_4(\text{ Bentone 34}) &= 5415 \\
 \text{Area of } i\text{-C}_4(\text{ Bentone 34}) &= 7740 \\
 \text{Area of } \text{C}_4^-(\text{ Bentone 34}) &= 1928 \\
 \text{Area of } i\text{-C}_4^-(\text{ Bentone 34}) &= 3300 \\
 \text{Area of } \text{C}_5^+(\text{ Bentone 34}) &= 5648
 \end{aligned}$$

From data of Shimadza GC 14B (Bentone 34 column)

Area of benzene (B)	=	5235
Area of toluene(T)	=	7658
Area of o-xylene(o-X)	=	1238
Area of m-xylene(m-X)	=	855
Area of p-xylene(p-X)	=	2235
Area of other(A <sub>9</sub> <sup>+</sup> )	=	3405

Selectivity of product is defined as mole of product (B) form with respect to mole of Ethanol converted:

$$\text{Selectivity of B (\%)} = 100 \times [\text{mole of B from/mole of Ethanol converted}]$$

Where B is product, mole of B can be measured employing the calibration curve of products such as benzene, toluene, o-xylene, m-xylene and p-xylene

$$\text{Mole of benzene} = (\text{area of benzene peak from integrator plot on GC-14B}) \times 10^{-10}$$

Hence: Product distribution (C-wt%)

C <sub>1</sub>	=	6.37
C <sub>2</sub>	=	1.19
C <sub>2</sub> <sup>=</sup>	=	4.25
C <sub>3</sub>	=	3.94
C <sub>3</sub> <sup>=</sup>	=	24.80
C <sub>4</sub>	=	7.22
i-C <sub>4</sub>	=	10.32
C <sub>4</sub> <sup>=</sup>	=	2.57
i-C <sub>4</sub> <sup>=</sup>	=	4.40
C <sub>5</sub> <sup>+</sup>	=	7.53
benzene (B)	=	6.98
toluene(T)	=	10.21
o-xylene(o-X)	=	1.65
m-xylene(m-X)	=	1.14

$$\begin{aligned} \text{p-xylene(p-X)} &= 2.98 \\ (\text{A}_9) &= 4.54 \end{aligned}$$

The other Ga/MFI catalysts were calculated same as the H/MFI ,which results are shown in Table C1



สถาบันวิทยบริการ  
จุฬาลงกรณ์มหาวิทยาลัย

**Table C1** Product distribution on ethanol aromatization with various particle sizes (a) fresh catalyts (b) pretreated catalyts

(a) fresh catalyts

Product	H/MFI (2 $\mu$ m)	0.5Ga/MFI (1 $\mu$ m)	0.5Ga/MFI (1.9 $\mu$ m)	0.5Ga/MFI (3.2 $\mu$ m)	0.5Ga/MFI (4.1 $\mu$ m)	0.5Ga/MFI (6.0 $\mu$ m)
c1	6.37	6.49	6.34	6.52	6.49	6.37
c1-4(p)	22.65	19.25	19.25	19.85	18.98	19.85
c1-4(o)	36.02	30.10	31.10	30.10	29.87	30.10
c5+	7.53	6.66	6.23	6.85	6.94	6.53
B	6.98	9.10	9.62	8.81	9.18	8.98
T	10.21	15.06	15.02	14.06	15.07	14.26
o-x	1.65	2.56	2.26	2.63	2.59	2.65
m-x	1.14	1.73	1.71	1.75	1.73	1.74
p-x	2.98	3.83	3.23	3.93	3.85	3.98
A9+	4.54	5.32	5.26	5.52	5.31	5.54

(b) pretreated catalyts

Product	H/MFI (2 $\mu$ m)	0.5Ga/MFI (1 $\mu$ m)	0.5Ga/MFI (1.9 $\mu$ m)	0.5Ga/MFI (3.2 $\mu$ m)	0.5Ga/MFI (4.1 $\mu$ m)	0.5Ga/MFI (6.0 $\mu$ m)
c1	6.67	6.49	6.34	6.52	6.49	6.37
c1-4(p)	27.65	20.16	21.01	20.85	20.98	20.95
c1-4(o)	39.59	31.10	32.90	32.10	31.87	33.42
c5+	8.29	7.66	7.23	6.85	6.94	6.53
B	2.18	8.98	7.35	6.01	5.68	4.21
T	7.26	14.06	13.97	13.06	12.55	11.26
o-x	1.25	2.36	2.53	2.78	2.89	3.94
m-x	0.96	1.23	1.71	1.65	1.73	1.84
p-X	1.98	3.03	3.73	4.28	4.96	5.81
A9+	4.14	5.12	5.26	5.02	5.31	5.64

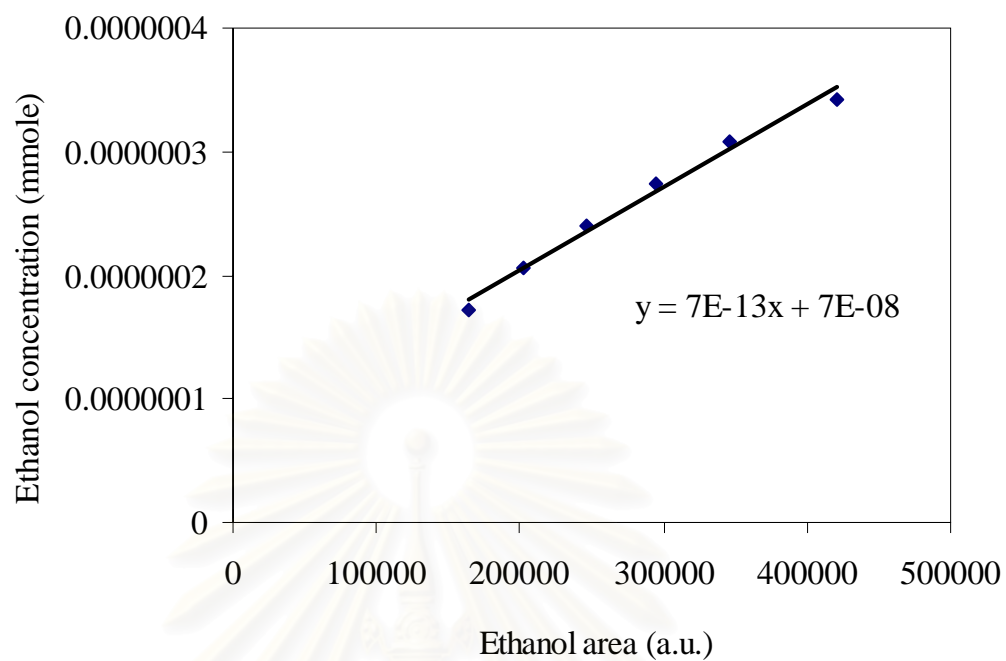


**Figure C1** Calibration curve of Ethanol.

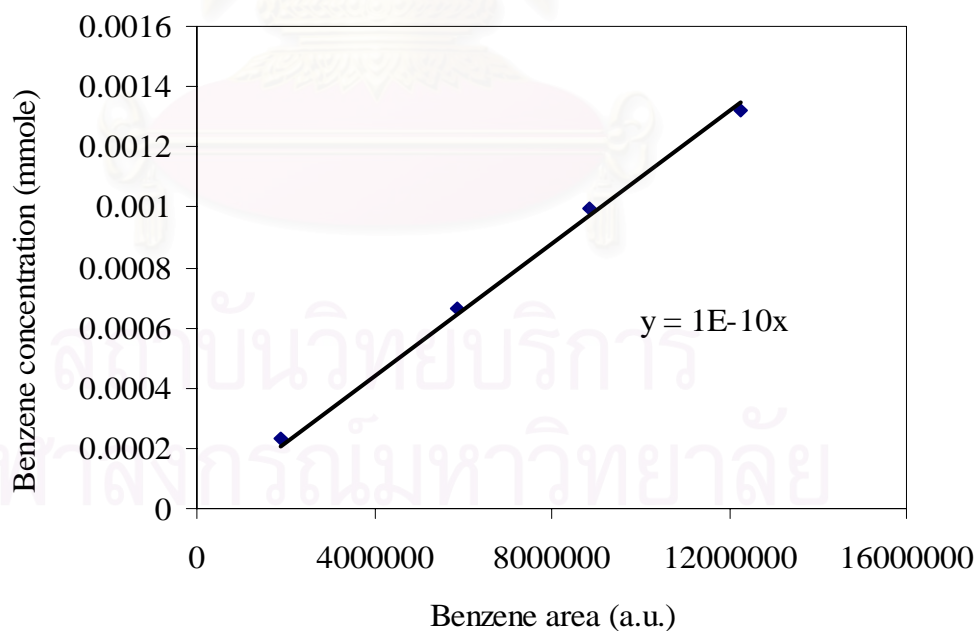


**Figure C2** Calibration curve of Benzene.

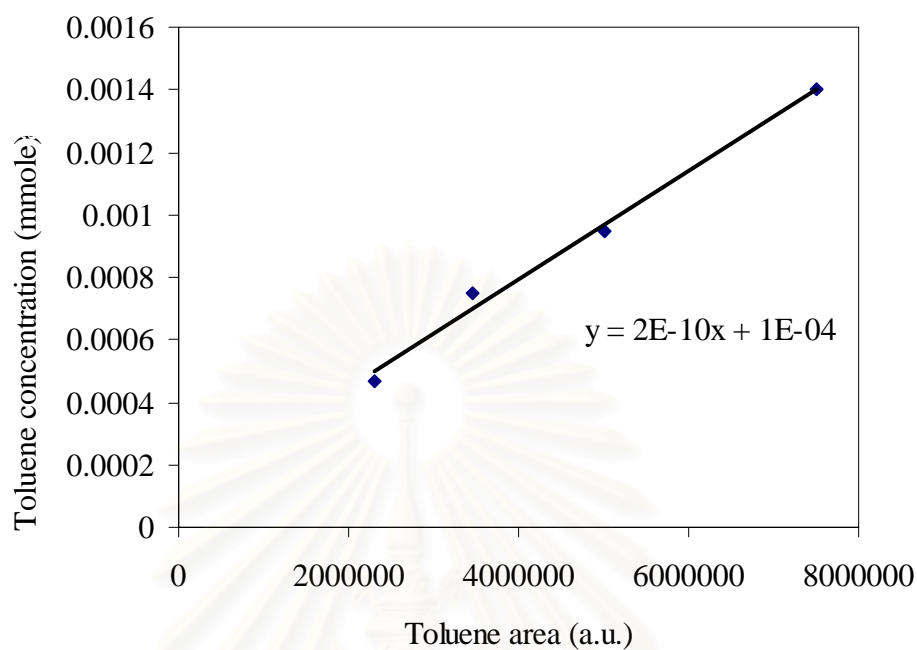


**Figure C3** Calibration curve of Toluene.

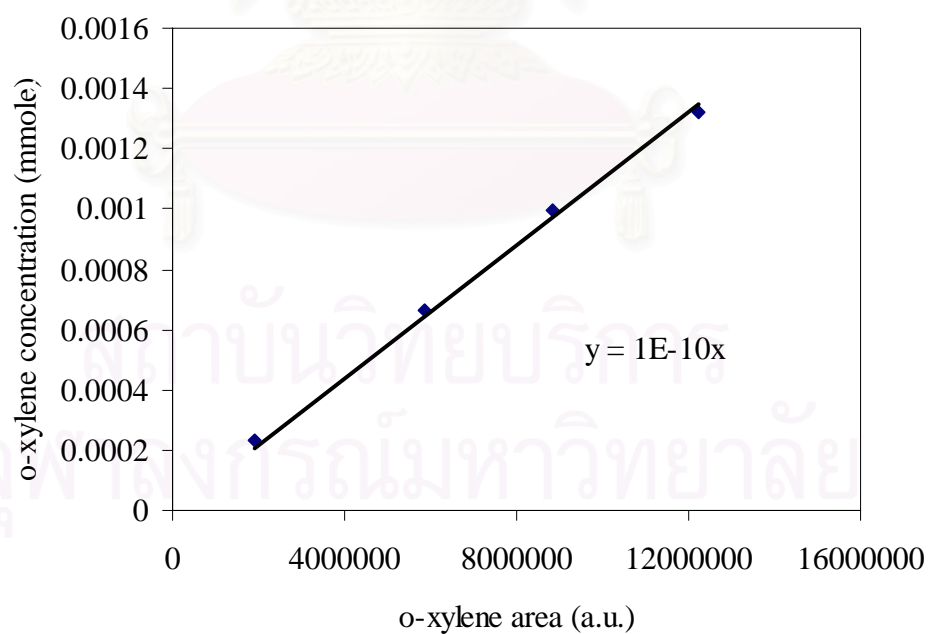


**Figure C4** Calibration curve of o-xylene.



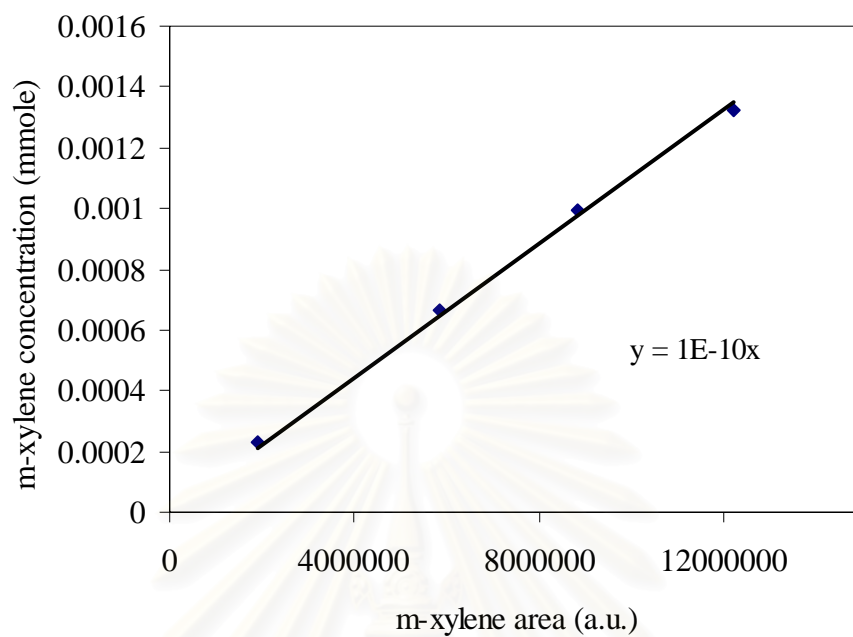


**Figure C5** Calibration curve of m-xylene.

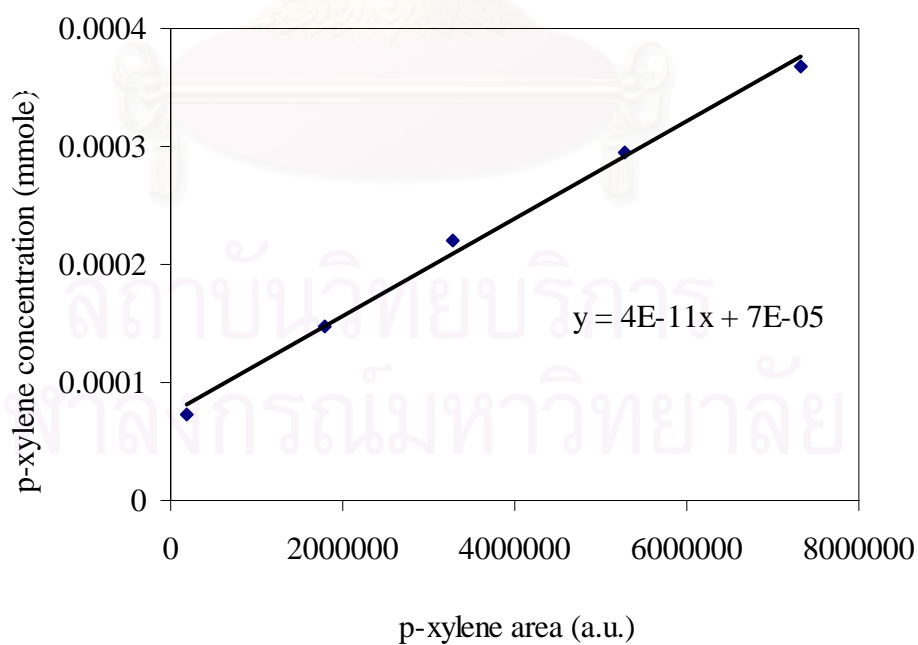


**Figure C6** Calibration curve of p-xylene.

## APPENDIX D

### LIST OF PUBLICATION

1. Paweenar Duenchay, Choowong Chaisuk, Suphot Phatanasri and Piyasan Prasertdam,” Effect of the crystal size of zeolite on the durability of Ga/HZSM-5 under hydrothermal condition”, Proceedings of the Thai Institute of Chemical Engineering and Applied Chemical Conference 15<sup>th</sup>, Chonburi, Thailand, Oct., 27-28, 2005, Ref. No CA-12



สถาบันวิทยบริการ  
จุฬาลงกรณ์มหาวิทยาลัย

# Effect of the crystal size of zeolite on the durability of Ga/HZSM-5 under hydrothermal condition

Paweenar Duenchay<sup>\*1</sup>, Choowong Chaisuk<sup>2</sup>, Suphot Phatanasri<sup>1</sup>  
and Piyasan Prasertthdam<sup>1</sup>

1) Center of Excellence on Catalysis and catalytic Reaction Engineering

Department of Chemical Engineering, Chulalongkorn University, Payatai Rd., Bangkok 10330, Thailand

2) Department of Chemical Engineering, Faculty of Engineering and Industrial Technology, Silpakorn University,  
Sanam Chandra Palace Campus, Nakorn Pathom 73000 Thailand

\* Presentor, Corresponding author (Tel: +66-02-2186766, Fax: +66-02-2186877, Email: paweenar13@hotmail.com)

## ABSTRACT

The effect of crystal size on the durability of Ga/HZSM-5 under hydrothermal condition was studied. The durability of the catalysts subjected to hydrothermal treatment with He stream containing 10% steam at 800 °C for 24 h was investigated. After the hydrothermal treatment, the crystallinity percentage for small crystal sizes (1.0 and 1.9 μm) was less decreased than that for large crystal sizes (4.1 and 6.0 μm). This implies that the durability of Ga/HZSM-5 increases with decreasing in crystal size.

Keywords: Ga/HZSM-5; Hydrothermal; Durability; Crystallinity

## 1. INTRODUCTION

ZSM-5 zeolite is a material of high interest, due to its well-known catalytic applications in a large number of chemical and petrochemical processes. In general, the ZSM-5 catalyst is usually loaded with another metal, to modify some properties of the synthesised catalyst. Several methods for loading another metal onto a catalyst exist, and ion-exchange method is one of them. ZSM-5 zeolites containing Zn or Ga ions are known to be effective in converting light alkanes into aromatics [2-3]. Furthermore these catalysts have been used in dehydrogenation, oligomerization and cyclization. Most reactions occur at high temperature coincident with the presence of water in process. The vapour generated during the reaction is an important problem of the use of these catalysts. Prasertthdam et al. [5] reported that the crystal size affects the durability of Co/HZSM-5 under hydrothermal treatment in selective catalytic reduction

of NO by methane. However, these studies have not been concerned with the durability of Ga/HZSM-5 catalysts. Thus, the aim of this work is to investigate the effect of crystal size of zeolite on the durability of Ga/HZSM-5 under hydrothermal treatment.

## 2. EXPERIMENTAL

### 2.1 Catalyst preparation

Four ZSM-5 catalysts, having different crystal sizes, however, with the same Si/Al ratio (Si/Al = 40) and Ga loading, were used in this work. The ZSM-5 was prepared according to the rapid crystallization method [4] using various crystallization rates. In order to transform the Na form of zeolite crystals into the NH<sub>4</sub> form, all samples were ion-exchanged with ammonium nitrate solution, washed, dried and then calcined at 540 °C for 3.5 h in air. Ga/HZSM-5 was subsequently prepared using an aqueous solution of

gallium nitrate for ion-exchange with HZSM-5 at 80 °C for 24 h. The Ga exchanged catalyst was washed, dried and calcined at 540 °C for 3.5 h in air.

In order to investigate the durability of the catalysts, they were heated under He atmosphere from ambient temperature to 800 °C with a heating rate of 10 °C/min and then kept at 800 °C for 24 h under 10 mol% of steam.

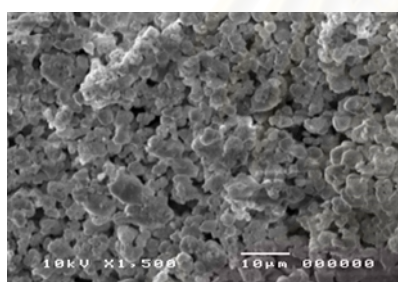
## 2.2 Catalyst Characterization

Specific surface areas of the catalysts was measured by physical adsorption based on BET assumption, with N<sub>2</sub> as the adsorbent using a Micromeritics model ASAP 2020. The crystallinity of the catalysts was determined using a X-ray diffractometer (SEIMENS D5000) with Cu K<sub>α</sub> radiation.

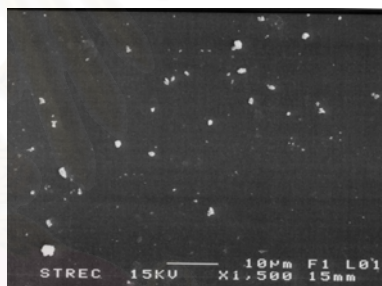
The percent crystallinity, as determined by XRD profiles, was calculated based on the main peak compared with the peak of the fresh that of HZSM-5 as a reference. The elemental compositions of the catalysts were determined by X-ray fluorescence spectroscopy (XRF). The morphology of the catalysts was observed using a scanning electron microscope (SEM, JEOL, JSM-35).

## 3. RESULTS AND DISCUSSION

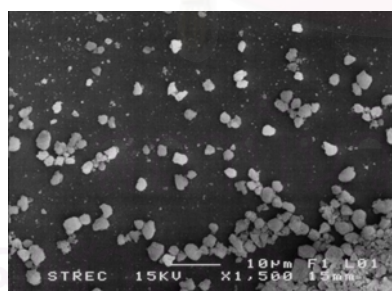
Table 1 shows the physical properties of the catalysts before and after pretreatment. Four ZSM-5 samples were selected as the parent ZSM-5. They have similar Si/Al and Ga/Al ratio but different crystal size from each other. The crystal sizes of the zeolite samples were measured by scanning electron



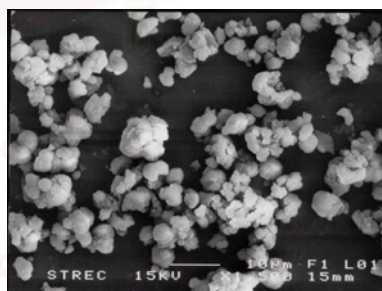
HZSM-5( 2.0 µm )



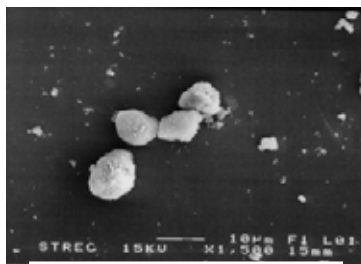
Ga/HZSM-5 ( 1.0 µm )



Ga/HZSM-5 ( 1.9 µm )



Ga/HZSM-5 ( 4.1 µm )



Ga/HZSM-5 ( 6.0 µm )

Fig. 1. Scanning electron micrograph of Ga/HZSM-5

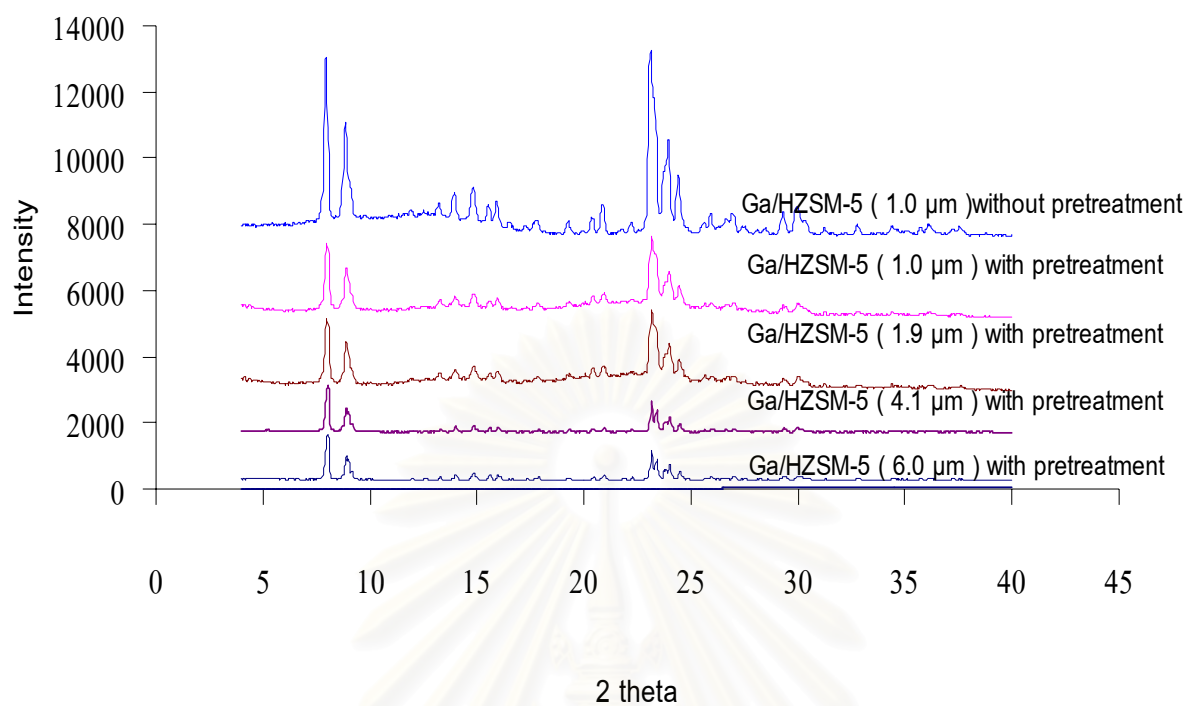


Fig. 2.XRD patterns of Ga/HZSM-5 without pretreatment and with pretreatment

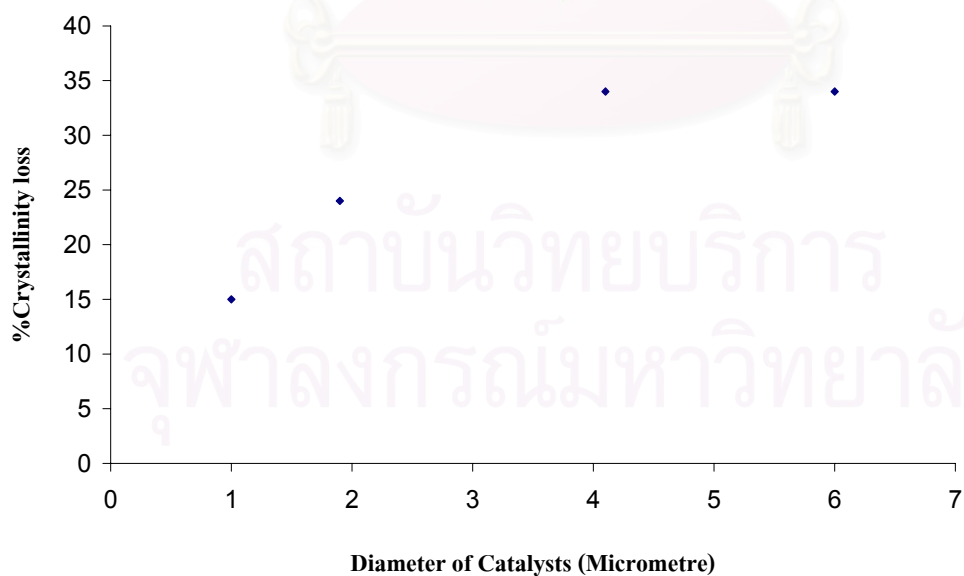


Fig. 3. The effect of crystal size on the %crystallinity loss of Ga/HZSM-5

micrographs averaging the diameter of a hundred primary particles based on the particle diameter. Crystal size values estimated from SEM images have been reported in many research articles [1,6,7]. The SEM photographs depicted in Fig.1 indicate that the diameters of Ga/HZSM-5 zeolites were 1.0, 1.9, 4.1 and 6.0  $\mu\text{m}$ .

The results shown in table 1 indicate that after hydrothermal treatment the BET surface areas of Ga/HZSM-5 (4.1 and 6.0  $\mu\text{m}$ ) significantly decreased, however, for the Ga/HZSM-5 catalysts with the small crystal size (1.0 and 1.9  $\mu\text{m}$ ), only a slight decrease in surface area was observed. According to XRD profiles of the fresh catalysts, the percent crystallinity of Ga/HZSM-5 (1.0 and 1.9  $\mu\text{m}$ ) was found to be higher than that of Ga/HZSM-5 (4.1 and 6.0  $\mu\text{m}$ ). It was also found that after ion-exchange of Ga into HZSM-5, Ga had no effect on the crystallinity of HZSM-5. After hydrothermal treatment at 800°C in 10 mol% steam for 24 h, no significant change in morphology of the samples was observed. As shown in fig 3, the Ga/HZSM-5 catalysts with large crystal size (4.1 and 6.0  $\mu\text{m}$ ) lost a considerable degree of their crystallinity after hydrothermal treatment. In contrast, for Ga/HZSM-5 (1.0 and 1.9  $\mu\text{m}$ ) only a slight decrease in crystallinity was observed upon hydrothermal treatment. Consequently, it appears definitely that the Ga/HZSM-5 catalysts with the small crystal sizes are more durable than those with the large ones on hydrothermal treatment with respect to crystallinity.

Table 1  
Physical properties of Ga/HZSM-5

Catalysts	Crystal diameter by SEM ( $\mu\text{m}$ )	Si/Al atomic ratio	Ga/Al atomic ratio	BET surface area ( $\text{m}^2/\text{g}$ )		%Crystallinity	
				Fresh	Pretreated	Fresh	Pretreated
HZSM-5 ( 2.0 $\mu\text{m}$ )	2.0	39.8	0.528	354	310	93	60
Ga/HZSM-5 ( 1.0 $\mu\text{m}$ )	1.0	38.6	0.530	309	306	94	79
Ga/HZSM-5 ( 1.9 $\mu\text{m}$ )	1.9	39.2	0.526	367	358	93	69
Ga/HZSM-5 ( 4.1 $\mu\text{m}$ )	4.1	40.7	0.551	333	314	98	64
Ga/HZSM-5 ( 6.0 $\mu\text{m}$ )	6.0	40.1	0.545	315	279	95	62

#### 4. CONCLUSION

The smaller crystal size Ga/HZSM-5 zeolite exhibited the greater durability for hydrothermal treatment condition. The smaller crystal size catalysts showed a slight decrease in crystallinity whereas the large crystal size catalysts lost considerable crystallinity.

#### REFERENCES

1. Budi P., Curry-Hyde E., Howe R.F. (1997), Stud. Surf. Sci. Catal. 105, 1549.
2. Choudhary V.R., Nayak V.S. (1982), Appl. Catal.4, 31
3. Choudhary V.R., Nayak V.S. (1982), Appl. Catal.4, 333
4. Inui T. (1989), ACS Symp. Ser. 389, 492.
5. Piyasan P., Nakarin M., Pornsawan K. (2002), Catalysis Communication 3, 191-197
6. Shichi A., Katagi K., Satsuma A., Hattori T. (2000), Appl. Catal. B 24, 97.
7. Tabata T., Ohtsuka H. (1997), Catal.Lett. 48, 203.



สถาบันวิทยบริการ  
จุฬาลงกรณ์มหาวิทยาลัย

## VITAE

Miss Paweenar Duenchay was born in April 13<sup>th</sup>, 1980 in Prachin-buri, Thailand. She finished high school from Benchamaratcharansarid School, Chachoengsao in 1999, and received bachelor's degree in Chemical Engineering from the department of Chemical Engineering, Faculty of Engineering, Suranaree University of Technology, Nakhon Ratchasima, Thailand in August 2003. She continued her Master study in the same major at Chulalongkorn University, Bangkok, Thailand in June 2004.



สถาบันวิทยบริการ  
จุฬาลงกรณ์มหาวิทยาลัย